THE EFFECTS OF CHRONIC AND ACUTE TOXICOLOGICAL EXPOSURES ON THE EXPRESSION OF THE TUMOR SUPPRESSOR *p16^{INK4a}*

Jessica Ann Sorrentino

A dissertation submitted to the faculty of the University of North Carolina at Chapel Hill in partial fulfillment of the requirements for the degree of Doctor of Philosophy in the Curriculum in Toxicology

Chapel Hill
2013

Approved by:

Norman E. Sharpless, MD

Rebecca Fry, PhD

Hyman Muss, MD

W. Kimryn Rathmell, MD

William Zamboni, PharmD, PhD

ABSTRACT

JESSICA ANN SORRENTINO: The effects of chronic and acute toxicological exposures on the expression of the tumor suppressor *p16*^{INK4a}
(Under the direction of Dr. Norman E Sharpless)

In mammals, expression of *p16*^{INK4a} is highly regulated. Excess expression can lead to cellular senescence and aging, while impaired activation is associated with cancer. The precise mechanism of *p16*^{INK4a} regulation *in vivo* is poorly understood. *In vitro* systems have limited utility since proliferation in culture induces *p16*^{INK4a}. Both extrinsic (chemotherapy and ionizing radiation) and intrinsic (telomere shortening and improper DNA damage repair) stimuli can induce *p16*^{INK4a}, but the kinetics of and cellular responses to these genomic insults have not been examined *in vivo*. To address this question, we developed a murine strain with firefly luciferase 'knocked-in' to the endogenous p16^{INK4a} locus and under control of the *p16*^{INK4a} promoter (*p16*^{LUC}).

To determine the expression of *p16*^{INK4a} after chronic exposure, we exposed *p16*^{LUC} mice to 50 ppm arsenic (As), 42% fat diet (HFD), 350 J/m^2 Ultraviolet B light (UVB), or cigarette smoke (CS) for a minimum of 6 months. Every other month, *p16*^{LUC} mice were imaged to measure luciferase induction. At 30 weeks of exposure, mice exposed to CS displayed 2 times higher levels of whole body luciferase activity than ambient air (AA) controls. Additionally, mice exposed to UVB exhibited 1.5 times higher levels of luciferase activity by 6 weeks of exposure that reached 8 times over control mice by 24 weeks. In As exposed mice, there was a slight, but statistically significant induction of *p16*^{INK4a} by 24

weeks. We observed no differences in $p16^{INK4a}$ expression in mice on HFD compared to normal diet (ND, 4%) after 78 weeks. We can deduce the direct DNA damaging agents, CS and UVB, are leading to an induction of $p16^{INK4a}$ while in direct DNA-damaging agents (e.g. As) cause a slight induction of $p16^{INK4a}$. However, non-DNA damaging agents, such as HFD, show no changes in expression when compared to ND controls.

To determine the regulation of transient $p16^{INK4a}$ expression, mice were exposed to a high dose of UVB light (2000 J/m^2). The mice were then imaged for luciferase induction at various time points over one month, allowing the burn to heal. To manipulate the induction of $p16^{INK4a}$ the mice were treated with pharmacological inhibitors, including dexamethasone (dex), clodrosome (clod), and compound A (cA). Dex, a known immunosuppression, showed a decrease in $p16^{LUC}$ expression, during the healing process along with clod, known to be toxic to macrophages, and cA, a p65 inhibitor. This data suggests that inflammation at the site of the burn can lead to the induction of $p16^{INK4a}$ through the recruitment of macrophages along the Nfκb pathway. The data generated from these experiments will demonstrate how environmental exposures are associated with expression of $p16^{INK4a}$, a mediator of tumor suppression and aging.

ACKNOWLEDGMENTS

I would like to express my appreciation and gratitude for Dr. Ned Sharpless with his guidance, mentorship, and support during my doctorial training. I would also like to thank my committee members Drs. Kim Rathmell, Hy Muss, Rebecca Fry, and Bill Zamboni for their time, expertise, and advice during my studies.

I could not have completed my doctorate degree without the generous support I received from my coworkers and scientific colleagues over the years. I would first like to thank my first principal investigator, Dr. Louis Trombetta, and my mentor Dr. Diane Hardej at St John's University, for sparking my interest in the toxicology field. My deepest appreciations go to the past and present members of the Sharpless and Dr. Billy Kim labs for their kind words and encouragement, particularly Dr. Krishnamurthy Janakiraman, Dr. Christin Burd, Dave Darr, Dr. George Souroullas, Dr. William Kim, Dr. Will Jeck, and Dr. Jim Alb. Several individuals of the Curriculum in Toxicology were instrumental in guiding me through this process, and I would especially like to acknowledge Dr. Marila Cordeiro-Stone, Dr. Ilona Jaspers, and Dr. Samantha Snow for their advice and support.

Finally, I would like to thank all of my wonderful friends, and amazing family for their never ending support and encouragement. Your unrelenting belief in me sustained me throughout this extensive process. I would especially like to acknowledge my parents Raymond Sorrentino and Teresa Sorrentino for instilling values and a strong work ethic in me, as well as my lifelong friends Seth Zimmerman, Jillian Weintraub, Ed Kahovec, and Ariel Edelson for listening, caring, and understanding during this experience.

TABLE OF CONTENTS

LIST OF TABLES

LIST OF FIGURES

LIST OF ABBREVIATIONS

8-OHdG	8-hydroxy-2'-deoxyguanosine
AA	Ambient air
ARF	Alternate reading frame of the INK4a/ARF locus
As	Arsenic
C. elegans	*Caenorhabditis elegans*
cA	Compound A
CAD	Coronory artery disease
CDKN2A	Cyclin-dependent kinase inhibitor 2A
Clod	Clodrosome
CS	Cigarette smoke
CXCL1	Chemokine (C-X-C motif) ligand 1
Dex	Dexamethasone
DNA	Deoxyribonucleic acid
Drosophila	*Drosophila melanogaster*
FOV-24	Field of view 24
GHR/BP$^{-/-}$	Growth hormone receptor/binding protein
Ghrhr$^{lit/lit}$	Growth-hormone-releasing hormone receptor
GROα	growth stimulating activity α
H2AX	Histone γH2A.X
HFD	High fat diet
HSF1	Heat shock factor protein 1
Igf1r$^{+/-}$	IGF-I receptor

IIS	Insulin/insulin-like growth factor signaling
IL-10	Interleukin 10
IL1α	Interleukin 1-alpha
IL-6	Interleukin 6
IL-8	Interleukin 8
J/m^2	Joules per meter squared
LTL	Leukocyte telomere length
MEFS	Mouse embryonic fibroblasts
mRNA	Messenger ribonucleic acid
ND	Normal diet
NDGA	Nordihydroguiaretic acid
NfκB	Nuclear factor *kappa*-light-chain-enhancer of activated *B* cells
$p/s/cm^2/sr$	Photons per second per centimeter squared per steradian
$p16^{LUC}$	$p16^{INK4a}$-luciferase
$p16^{TOM}$	$p16^{INK4a}$-tdtomato
PBTL	Peripheral blood T-lymphocyte
PNCA	Proliferating cell nuclear antigen
ppm	Parts per million
RB	Retinoblastoma protein
SA	Senescence associated
SASP	Senescence associated secretory phenotype
SA-β gal	Senescence associated β galactosidase
TBLI	Total body luciferase imaging

TM	Telomere maintenance
UV	Ultraviolet light
UVB	Ultraviolet B light
Zebrafish	*Danio rerio*

CHAPTER 1: INTRODUCTION

Aging is a complex process with contributions from both genetic and environmental factors. There has been a great effort to determine how environmental agents are carcinogenic, but very few studies have been done to show how long term exposures can lead to aging (Goldsworthy et al., 1994; Jacobson-Kram et al., 2004). Long term studies, independent of research goal, are extremely costly, with time and mice very expensive (Long et al., 2010). Many groups have started to move towards more *in vitro* (e.g. ToxCast) models for their high throughput nature, however *in vitro* models cannot answer most physiological questions (Dix et al., 2007). A critical need in gerontologic research is an understanding of how host genetics and environmental exposures interact over the organismal lifespan to produce common phenotypes of aging such as increased risk to certain diseases, loss of regenerative capacity and frailty.

Aging and Senescence

Mammalian aging results from multiple distinct processes and it is unlikely that any single pathogenic pathway accounts for all aspects of aging. While disparate molecular pathways surely contribute, several lines of evidence suggest the activation of cellular senescence is an important contributor to many age associated conditions. Moreover, the

accumulation of senescent cells *in vivo* appears to be measurable, providing a means to determine if a noxious exposure or toxicant accelerates this aspect of aging. This research will give us insight to the mechanisms of aging after toxicological exposure.

Cellular Senescence and *p16^{INK4a}* Expression

Senescence is the state at which cells stop dividing and reach their proliferative capacity, known as the Hayflick limit (Hayflick and Moorhead, 1961). There are specific factors that define a senescent phenotype, as reviewed in (Rodier and Campisi, 2011). These factors include, but are not limited to: a permanent growth arrest, an enlarged cellular size, altered gene expressions (*p21^{CIP}*, *p16^{INK4a}*, *C-fos*, *PCNA*), increase SA-β-galactosidase (SA β-gal) staining, and senescence associated secretory phenotype (SASP) (Figure 1). Even though these cells do not replicate, they remain metabolically active. Recent evidence has shown that cellular senescence is supplemented with a marked increase in the secretion of a wide-range of factors including, proteases, chemokines and cytokines, most known to stimulate inflammation, known as SASP. Many components can influence cellular senescence. Factors that cause senescence include telomere shortening, induction of oncogenes (Serrano et al., 1997; Zhu et al., 1998), oxygen radicals (Chen et al., 2004), DNA damage (Bartkova et al., 2006; Meng et al., 2003), and epigenetic silencing (Chen et al., 2009). For example, prior *in vivo* work has shown that whole body ionizing radiation, a known damaging agent, will lead to senescence in the hematopoietic stem cells (Wang et al., 2006). Furthermore, mounting evidence has shown that a known tumor suppressor, *p16^{INK4a}*, is not only a mediator of senescence after exposure (e.g. ionizing radiation) but also a

biomarker for aging (Janzen et al., 2006; Krishnamurthy et al., 2006; Krishnamurthy et al., 2004; Liu et al., 2009; Molofsky et al., 2006).

$p16^{INK4a}$ is a cell cycle inhibitor and part of the retinoblastoma protein (RB) pathway along with other RB-family proteins (p107, p130). In a normal cycling cell, cyclin D/CDK4/6 complex will bind to the RB protein, allowing RB to hyperphosphorylate. The hyperphosphorylated RB protein will then release the E2F transcription factor. Once the E2F transcription factor is released, the cell will move from the G1 to S phase of the cell cycle. When $p16^{INK4a}$ is activated, the protein will physically block cycle D from binding to CDK4/6, causing RB to stay bound to E2F. Without the release of E2F, the cell will pause between G1 to S phase (Figure 2). It is still unclear how the cell decides move from a quiescent (transient growth arrest) to senescent state (permanent growth arrest). Recent discoveries have given insight as to the regulators of $p16^{INK4a}$. One group has should that $p16^{INK4a}$ locus is H3K27-methylated and bound by BMI1, RING2, and SUZ12 leading to transcriptional repression of the transcript (Kotake et al., 2007). Others have shown that EZH2 is down-regulated in senescing cells, along with displacement of BMI1, and activation of $p16^{INK4a}$ expression (Bracken et al., 2007). Additionally, through downregulation of $p16^{INK4a}$ and ARF, overexpression of BMI-1 will lead to fibroblast immortalization, and with the addition of H-ras activation it will lead to malignancy in mice (Jacobs et al., 1999). Lastly, prior work has demonstrated that in senescent cells, the increase in $p16^{INK4a}$ expression is correlated with the decrease of Id1 and accumulation of Ets1 (Ohtani et al., 2001). While the immediate upstream transcription factors have been discovered, however, relationship between environmental exposure and modulation of transcription factors remains unclear. Even though the research has made tremendous advances in understanding the

molecular mechanisms of $p16^{INK4a}$ regulation with respect to cancer and aging, there are still many questions that need to be answered.

In vitro, $p16^{INK4a}$, along with other proteins including ARF, is strongly associated with senescence. Prior work has shown that oxidative stress of many primary mammalian cell types, including WI38 (human fibroblasts) and mouse embryonic fibroblasts (MEFs), will lead to the induction of $p16^{INK4a}$, and eventually lead to senescent state. Consequentially, if $p16^{INK4a}$ is suppressed, the cells will transform allowing for infinite passages, a neoplasmic phenotype. This same phenotype has been shown with ARF, a similar cell cycle regulator located along with $p16^{INK4a}$ on the *CDKN2A* locus (Matheu et al., 2008). Additionally, when cells are transformed with an oncogene (termed 'oncogene induced senescence'), there is a robust induction of cells cycle inhibitors including $p16^{INK4a}$, further validating the relationship between $p16^{INK4a}$ and senescence. Moreover, cells with high levels of $p16^{INK4a}$ are shown to be cancer resistant (Matheu et al., 2004). By preventing proliferation of a cell harboring DNA damage or oncogene activation, the senescence pathway is a pivotal tumor suppressor mechanism. (Campisi and d'Adda di Fagagna, 2007; Sager, 1991).

Organismal Aging

$p16^{INK4a}$-mediated senescence is currently believed to contribute to mammalian organismal aging through at least two mechanisms. First mechanism is through senescence-mediated loss of replicative capacity at the level of the tissue stem cell. This loss leads to impaired homeostasis and regenerative capacity in response to stressors including DNA damage and oncogene activation (Sharpless and DePinho, 2007). Initially findings showed

that senescent cells accumulate with aging *in vivo* (Dimri et al., 1995). Moreover, activation of $p16^{INK4a}$ and senescence has been linked to replicative hypofunction in several tissues (i.e. neural stem cells (Molofsky et al., 2006), hematopoietic progenitors (Janzen et al., 2006), lymphocytes (Liu et al., 2009; Signer et al., 2008), and pancreatic β-cells (Krishnamurthy et al., 2006)). Notably, this replicative hypofunction that comes with increased $p16^{INK4a}$ expression with aging is markedly attenuated in the absence of $p16^{INK4a}$ suggesting a causal relationship. Further evidence that the senescence pathway plays a vital rule in human aging includes correlation of senescence associated markers (e.g. $p16^{INK4a}$, *COX-1*, *COX-2*, SA β-gal) expression with chronological age in skin, kidney, and PBTLs (Dimri et al., 1995; Liu et al., 2009; Melk et al., 2004). Prior Altered regulation of the senescence promoting CDKN2a/b locus, which encodes $p16^{INK4a}$, $p15^{INK4b}$ and ARF, has been linked to age-associated phenotypes including atherosclerotic disease, type II diabetes, glaucoma and several malignancies (Jeck et al., 2012).

The second mechanism whereby senescence may contribute to phenotypic aging may be through the effector molecules of SASP. More specifically research has demonstrated that the release of Il-6, a marker for inflammation, has been shown to increase in senescence cells (Freund et al., 2010; Grivennikov et al., 2009; Hodge et al., 2005; Kuilman et al., 2008). *In vivo*, many SASP factors including Il-6, Il-10, Il-8, Il-1a, Groα, are associated with both lack of cellular regeneration and hyperproliferation in mice and humans (Coppe et al., 2010; Davalos et al., 2010; Liu et al., 2009). In fact, SASP factors have been shown to promote tumorigenesis in some cancers including mammary (Krtolica et al., 2001), melanoma (Lazar-Molnar et al., 2000), and prostate (Yang et al., 2005). These similarities may be due to the common low-grade inflammation found during both aging and tumorigenesis (Bruunsgaard

et al., 2001). Pharmacologic and genetic approaches to manipulate the number of senescent cells *in vivo* can ameliorate age-associated phenotypes such as sarcopenia, kyphosis, and hypo-replication of T-lymphocytes and pancreatic β-cells (Berent-Maoz et al., 2012; Chen et al., 2011a; Zindy et al., 1997). One group has generated a murine model that allows drug-inducible elimination of $p16^{Ink4a}$-positive senescent cells. After induction, the tissues (e.g. adipose, skeletal muscle and eye) that have $p16^{INK4a}$-dependent age-related disease have delayed onset of these phenotypes with removal of $p16^{INK4a}$-expressing cells (Baker et al., 2011).

The Science of Biological Aging

Historically, there has been immense effort to understand the genetics of aging across species. Many transcription factors found in *Caenorhabditis elegans* (C. elegans) have been shown to promote longevity including HSF-1 and DAF-16 (Hsu et al., 2003). Additionally, extended lifespan of *Drosophila melanogaster* (Drosophila) is exhibited after overexpression of protein carboxyl methyltransferase (PCMT), a protein repair enzyme (Chavous et al., 2001). Collaboratively, comparative analysis of DNA microarray experiments has shown a common pattern of aging regulation among species including C. elegans and Drosophila (McCarroll et al., 2004). In murine models, there has been immense work to affect lifespan through genetically manipulation. Some of these alleles include, the 'little mouse' ($Ghrhr^{lit/lit}$), mice null for either growth hormone receptor/binding protein ($GHR/BP^{-/-}$) or p66shc ($p66shc^{-/-}$), mice heterozygous for the IGF-I receptor ($Igf1r^{+/-}$), and fat-specific insulin receptor knockout mice (Liang et al., 2003). Human studies have also a genetic link with lifespan. Genome-wide associated studies indicate that SNPs in the insulin/insulin-like

growth factor signaling (IIS) pathway and the telomere maintenance (TM) pathway are associated with human longevity (Deelen et al., 2013). Aging genetics has been well-established; however there are still answers that are necessary for understanding environment effects of aging.

Some aspects of toxicological aging, including DNA damage and diet, have been studied in species other than mammals, such as *Danio rerio* (zebrafish). For example, reactive oxygen species (ROS) formation induced by copper exposure is responsible for the increase in DNA repair gene expression, a known effector of aging (Sandrini et al., 2009). Exposure of zebrafish larva to oarathyroid hormone resulted in net bone loss, another common age related disease (Fleming et al., 2005). Additionally, long-lived zebrafish mutants show increase resistance to oxidative damage (Gruber et al., 2009). Dietary caloric restriction has shown to increase lifespan in many organisms including drosophila (Frankel et al., 2011), C. elegans (Gerhard and Cheng, 2002), and mice (Masoro, 2000; Sohal et al., 1994). The minimal work that has been done in mammals has largely focused on the pharmacology of aging. Rapamycin, an inhibitor of the mTOR pathway, has been shown to extend the lifespan of mice when given later in life (Harrison et al., 2009). Rapamycin treated mice also show slower age-related changes in heart, liver, adrenal glands, endometrium, and tendons (Wilkinson et al., 2012). The National Institute on Aging's Interventions Testing Program has completed a study testing four candidate agents for potential aging-delaying compounds, in hopes to understand the mechanism of aging after environmental exposure. Even though none were successful for extending lifespan, nordihydroguiaretic acid (NDGA) reduces early life mortality risks (Miller et al., 2007). In

summary, there has been some work to show the relationship between exposures and aging in numerous species, however little research has been focused on mammalian aging toxicology.

Gerontogens

In 1987, George Martin pointed out that the rate of aging is largely non-genetic (>50%), and coined the term "gerontogen" to describe an environmental agent that accelerates aging. In response to gerontogen exposure, phenotypic outcomes at the organismal level include the loss of proliferative homeostasis, the decline in the efficiency of enzyme adaptation, and immunodeficiency (Martin, 1987). Martin also discusses categories of environmental gerontogens including segmental gerontogens, which affect multiple senescent phenotypes, and unimodal gerontogens which affect only a specific tissue or organ. Environmental exposures (or therapeutic exposures such as radiation and chemotherapy) act as gerontogens when they lead to cellular insults that induce, what is now considered, cellular senescence (e.g. DNA damage or increasing reactive oxygen species). According to this theory, differential exposure to gerontogens may underlie the marked phenotypic variation in human physiological aging (Figure 1).

<u>High Fat Diet</u>

Research has shown that high fat diet can lead to certain age related diseases including diabetes, atherosclerosis, and cancer in both humans and mice, making it a potential gerontogen (Giovannucci and Goldin, 1997; Purcell-Huynh et al., 1995; Schulze et al., 2004; Tannenbaum, 1942; Winzell and Ahren, 2004; Xu et al., 2001). Specifically, lack of cellular proliferation is seen in the pancreatic β-cell in high fat induced diabetic mice

(Sone and Kagawa, 2005). Additionally, prior studies on the effects of obesity and high fat diet (HFD) on $p16^{INK4a}$ expression, a cell cycle inhibitor and known marker for senescence, *in vivo* have given very tissue specific results. For example, HFD has been reported to increase senescence and $p16^{INK4a}$ expression in the murine aorta (Wang et al., 2009), whereas $p16^{INK4a}$ mRNA expression in peripheral blood T-lymphocytes (PBTL) does not correlate with body-mass index, a marker of obesity, in humans (Liu et al., 2009). High fat diet can be considered a gerontogen, however the mechanism of its advanced aging phenotype, is less certain. It is well known that fat causing an induction of reactive oxygen species, which can lead to a senescent phenotype (Tchkonia et al., 2010). One question that remains unanswered is which senescent pathway leads to the advanced aging phenotype *in vivo*.

Arsenic

Arsenic is a non-DNA damaging gerontogen. It is a common toxicant found in ground water that has been linked to age-related phenotypes including cancer (e.g. skin, bladder), type II diabetes, and atherosclerosis (Kapaj et al., 2006). Others have shown that arsenic among other heavy metals can leads to many age-related neurodegenerative diseases, including Alzheimer's disease, Parkinson's disease, Huntington's disease and Ataxia telangiectasia (Migliore and Coppede, 2009). While genetic background plays a role with some of these neurodegenerative disorders, exposures to arsenic can accelerate the pathology.

While arsenic does not directly damage DNA, there is substantial evidence that arsenic induces oxidative genotoxicity as well as hinders that function of DNA repair machinery (Andrew et al., 2003; Hartwig et al., 1997; Yamauchi et al., 2004). In mice, there

are more of 8-hydroxy-2'-deoxyguanosine (8-OHdG) adducts, a marker for oxidative DNA damage, in the brain of mice that were exposed to as little as 1 or 2 ppm of arsenic, which lead to degeneration of the cerebral and cerebellar cortexes (Piao et al., 2005). In humans, there is a positive association between arsenic concentrations in whole blood with the level of reactive oxidants in plasma (Wu et al., 2001). In both rodents and humans, arsenic decreases the functionality of DNA repair machinery. One study completed in rats, shows that after exposure to sodium arsenite, rats were challenged with benzo(a)pyrene to promote DNA damage repair. The results show that rats exposed to the arsenic incorporated less ^{32}P, suggesting a slower efficiency of DNA repair (Tran et al., 2002). Studies in humans show similar results. One study measured a cohort of citizens from West Bengal, India, a common hot spot for high levels of arsenic in the drinking water. DNA damage and chromosomal aberrations were found to be significantly higher in the arsenic-exposed individuals compared to unexposed individuals. Additionally, the challenge assay showed that upon induction of DNA damage, the repair capacity in the exposed individuals with premalignant hyperkeratosis is significantly less than that of individuals without skin lesion within the arsenic exposed group (Banerjee et al., 2008). Another study showed that arsenic exposure was associated with decreased expression of ERCC1, a known protein involved in nucleotide excision repair, in lymphocytes from a cohort in New Hampshire, USA and Sonora, Mexico at the mRNA and protein levels (Andrew et al., 2006). The gerontogenic effects of arsenic may be due to the induction of oxidative DNA damage as well as the decrease in DNA damage repair efficiency.

UV Light

Ultraviolet light is a potential unimodal gerontogen since almost all age-related pathologies are associated with the skin. There is strong evidence to correlate the effects of UV leading to photoaging and skin cancer (Kligman, 1989; Scharffetter-Kochanek et al., 2000). Additionally, prior work has suggested that acute UVB exposure can rapidly induce senescence in human skin (Pavey et al., 1999). Others have also shown that chronological aging and photoaging share basic molecular mechanisms including inductions of cytokines, ROS, UV-associated transcription factors (e.g. AP-1). Moreover, UV-induced ROS cause negative effects on cellular components including DNA, proteins, lipids, which is similar to a chronological aging phenotype (Fisher et al., 2002).

There is substantial evidence showing how UV light causes direct DNA damage. As far back as 1966, research has shown that UV light leads to pyrimidine dimers in DNA (Setlow and Carrier, 1966). Others show that the DNA damage can cause changes in age-related markers including the induction of SASP factors (Il-6, NFκB) (Freund et al., 2011; Rodier et al., 2009), and tumor suppressor genes ($p16^{INK4a}$, ARF, p53) (Bartkova et al., 2006; Lakin and Jackson, 1999) as well as a strong relationship between the mechanisms of age related telomere decay and DNA damage checkpoint (d'Adda di Fagagna et al., 2003). In addition to direct DNA damage, UV light, specifically UV-B light, causes ROS-associated DNA damage potentiating the aging phenotype (Cadet et al., 2005; Wei et al., 1998). Both indirect and direct DNA damage are responsible for the gerontogenic properties of UV light.

Cigarette Smoke

One common segmental, or multifaceted, gerontogen is cigarette smoke. Exposure to both primary and secondary smoke can lead to a vast array of aging phenotypes, which include advance aging of the skin, bones, and teeth as well as deleterious effects of the reproduction, cardiac, and pulmonary systems, and extensive cancers to the head, neck, and lungs (Bernhard et al., 2007). In addition to its well-known impact upon various types of neoplasms, it also had deleterious effects upon reproduction, the cardiovascular and pulmonary systems, skin, and bone diseases such as emphysema, atherosclerosis and several cancers (Bernhard et al., 2007; Ito and Barnes, 2009). The relationship with chronological age was much more striking, but it remains to be seen if there is any causal relationship to mechanisms of aging.

The mechanism of action for cigarette smoke is very complex, due to the extensive amount of chemicals found in a cigarette, including formaldehyde, carbon monoxide and nicotine. Research shows that mutagens in cigarette smoke promote DNA damage (DeMarini, 2004; Pfeifer et al., 2002) as well induce neurodegeration (Slikker et al., 2005), which are also potential mechanisms of gerontogenesis. More specifically, both formaldehyde and nicotine can accumulate in the brain leading to an age-dependent cognitive decline in rats (Belluzzi et al., 2004; Tong et al., 2013). Additionally, cigarette smoke led to decreased exhaled nitric oxide, suggesting a potential mechanism for age-related increased risks of chronic respiratory and cardiovascular disease in cigarette smokers (Kharitonov et al., 1995). In humans, our group and others have shown chronic cigarette smoke exposure in

humans is associated with increased *p16*^{INK4a} expression and shorter LTLs in PBTL (Liu et al., 2009; Mirabello et al., 2009; Nelson et al., 2012; Song et al., 2010; Valdes et al., 2005).

Measuring aging and senescence

Some of the markers of cellular senescence that increase with aging in humans and mice include SA β- galactosidase staining [48], SASP factors [49], telomere foci [50], and expression of the p16^{INK4a} tumor suppressor gene [13, 46, 51, 52] (Table 1). While all have shown an increase in specific experiments, very few are substantial, global, consistent, increase in many organs over time. Historically, SA β-galactosidase staining has been used to measure senescence, since senescent cells have been shown to have higher levels of endogenous β-galactosidase expression due to a lower pH. *In vitro*, this marker is very consistent; however *in vivo* interpretation can be difficult. Since SA β-gal stain is based on a change in pH, the differences in pH can change between tissues as well as throughout a singular tissue, making the results convoluted. SA β-gal stain is also poorly suited as a longitudinal translational measure of aging because of the requirement for end-organ staining. In murine studies the animal needs to be sacrificed for proper analysis, and human studies are not feasible with rare exception because of need to biopsy.

In humans, telomere length has been associated with chronological age. For example, decreased leukocyte telomere length (LTL) has repeatedly found to be inversely correlated with chronological age, anticipated 25 basepairs per year (Chen et al., 2011b; Lin et al., 2010). Further, average LTL is shorter in people with known exposure to gerontogens including cigarette smoking and obesity (Mirabello et al., 2009; Song et al., 2010; Valdes et al., 2005). Unfortunately, LTLs are difficult to use as a biomarker for in depth studies since

confounding factors of physiological aging in humans make it difficult to control. First, despite the long held conception that telomere length is a marker for residual replicative capacity (e.g. cells with shortened telomeres will not be able to replicate), there is little evidence to substantiate that hypothesis in humans (Longo, 2009). In fact, in one of the most highly replicative organs the bone marrow in which aging is known to lead to marrow dysfunction, LTL does not predict circulating levels of leukocytes, erythrocytes or platelets, therefore does not predict the replicative capacity of their progenitors(Mollica et al., 2009). Second, while telomere length will decrease across the lifespan in population-based studies, LTL varies substantially among individuals of the same age, and the absolute change is relatively small over an organism's lifespan it is unlikely to be a reliable aging biomarker (Longo, 2009; Muezzinler et al., 2013; Valdes et al., 2005). Additionally, the methods for determining LTL are difficult and expensive, making it less appealing as a high throughput biomarker.

IL-6, a pro-inflammatory cytokine, is also associated with aging. In large cohort studies, IL-6 increases with age. IL-6 is implicated causally in the aging process as the cause of a chronic inflammatory state that leads to age-associated debility (Hager et al., 1994; Maggio et al., 2006). In addition, elderly individuals with physical frailty and disability have higher IL-6 than those with lower levels (Cesari et al., 2004; Cohen et al., 1997; Taaffe et al., 2000). Despite these associations, IL-6 is poorly suited as a biomarker of physiological age in studies of potential gerontogens. In healthy adults IL-6 is commonly either below or at the lower limits of detect, yet dramatically increases during acute illness, making LTL levels extremely variable. IL-6 also has strong cyclical associations with the circadian rhythm (Ershler and Keller, 2000; Maggio et al., 2006). IL-6 may be a key part of a chronic

inflammatory milieu that causes physical decline with aging, but it is poorly suited as an outcome measure of the effect of environmental exposures on aging in humans.

Expression of $p16^{INK4a}$ in PBTLs has been shown to a faithful biomarker for chronological age, due to a stable, dynamic increase over a lifespan, in many different organs in both humans and mice [13, 52](Table 1). Because of the ability to measure $p16^{INK4a}$ in people with the CD3+ T-lymphocyte assay, these exposures can be evaluated in people. In humans, known DNA damaging chemotherapy treatments lead to higher levels of $p16^{INK4a}$ expression in the T cells of patents after treatment. While there are some limitations for $p16^{INK4a}$ expression including difficultly to solate T-lymphocytes, this biomarker seems to be a promising candidate for in clinic evaluation of aging.

Measuring toxicological aging *in vivo*

Recently, a new p16-luciferase ($p16^{LUC}$) allele developed in Norman Sharpless' lab, allowing the field of aging to begin testing the rate of aging *in vivo*, while decreasing cost and time, thus opening the door to a promising biomarker for *in vivo* testing after exposure to gerontogens. For this allele, firefly luciferase is knocked into exon 1α immediately after the start codon in the *Cdkn2a* locus. With the knock-in specific to exon 1α, the ARF construct, which consists of exon 1β, 2, and 3, remains functional. The Sharpless group has published a paper, showing the reporter allele faithfully measuring *in vivo* induction of $p16^{INK4a}$ in correlation with chronological age (Burd et al., 2013)(Figure 3). The major benefit of this allele is that the mice can be serially imaged decreasing cohort size, while gathering data at an individual level. Others have shown that caloric restriction and exercise are known to decrease the rate of aging over time, specifically $p16^{INK4a}$-associated gerontogens, such as

cigarette smoke, induce $p16^{INK4a}$ expression at a faster rate when compared to non-exposed cohorts in both human PBTLs and whole mice (Krishnamurthy et al., 2004; Liu et al., 2009). Specifically, $p16^{INK4a}$ increases at a faster rate over time in chronic smokers when compared to both former and non-smokers in human PBTL (Liu et al., 2009). In mice, $p16^{INK4a}$ expression is much higher in the upper respiratory region after four months of exposure to low chronic dose of cigarette smoke. Using the $p16^{LUC}$ mice, other gerontogens enhance the $p16^{INK4a}$-associated aging rate include UV light and to a lesser extent arsenic, further confirming the value of this reporter allele.

Aging is a dynamic, complex process that encases many mechanistic pathways, making it challenging to objectively measure. Further, the field of aging has made great progress in understanding the genetics of aging, but to a lesser extent the toxicological effects of aging. My work uses a novel allele to quantitatively measure $p16^{INK4a}$ associated aging in an unbiased manner. Moreover, my work contributes to mechanistically understanding how environmental exposures can lead to an advanced aging phenotype.

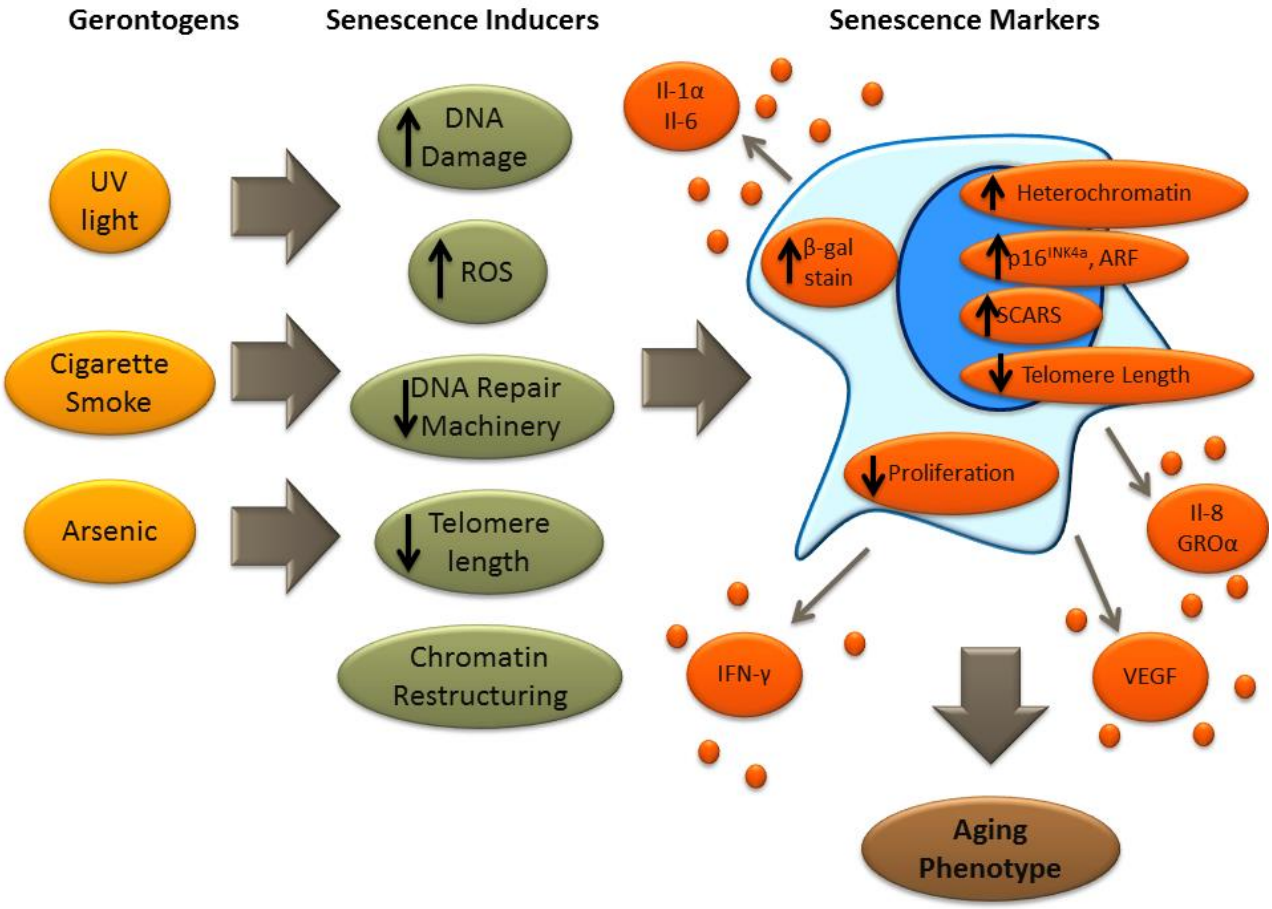

Figure 1.1: Summary demonstrating known gerontogens, mechanistic inducers of senescence and biomarkers of a cellular senescent phenotype

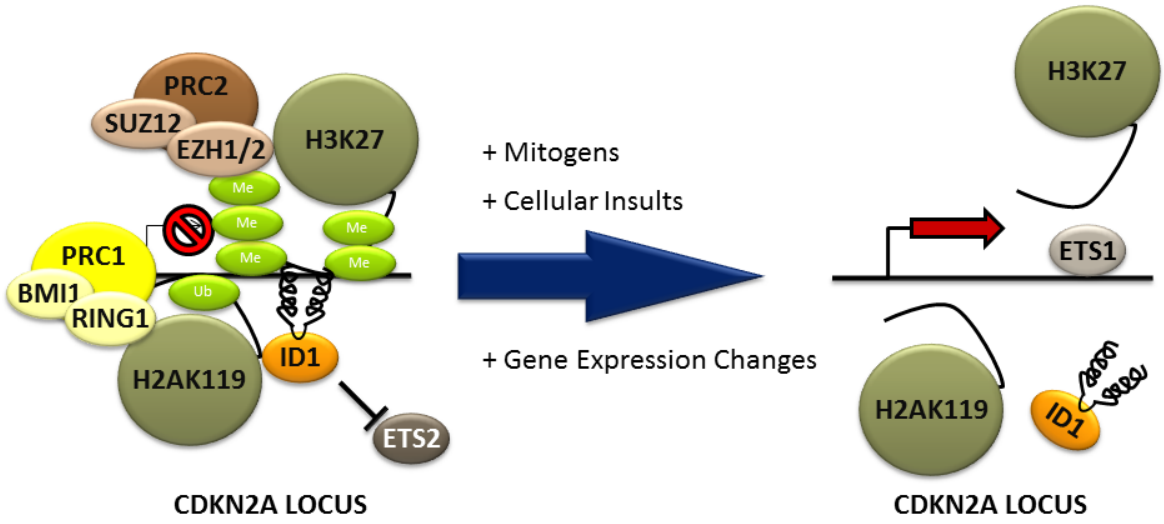

Figure 1.2: Schematic of *p16*^{INK4a} transcriptional regulation

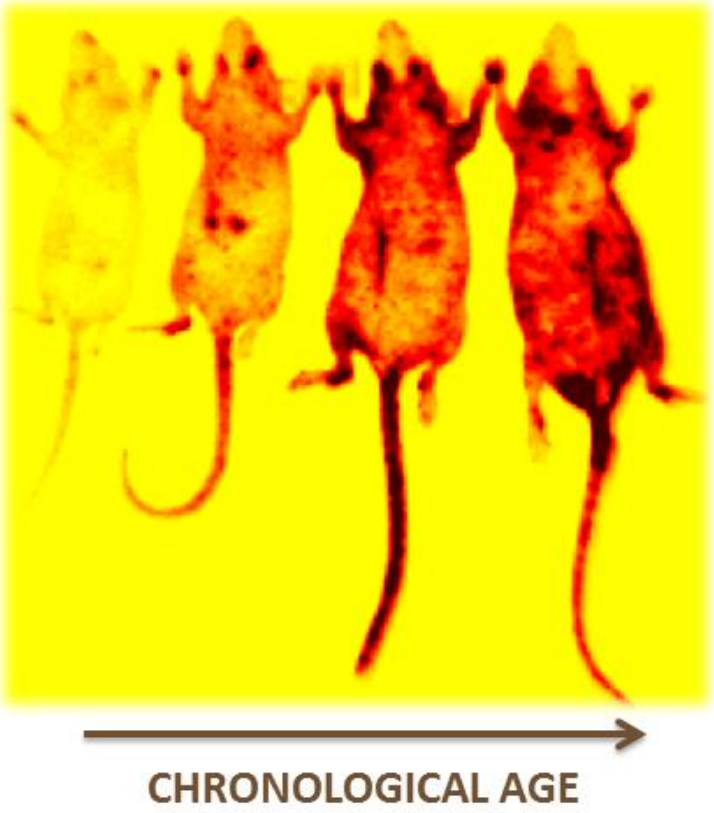

Figure 1.3: Increased expression of *p16^{INK4a}* , or increased luminescence signal, in *p16^{LUC}* aging mice demonstrating the relationship between *p16^{INK4a}* and aging *in vivo*.

Biomarker	Strengths	Weaknesses
Senescence Associated β-galactosidase stain	- Widely used - Consistent results *in vitro*	- Varies across/within tissues *in vivo*
SASP Marker, Il-6	- Straightforward assay - Consistent with population analysis	- Inconsistent for individual analysis - Uncontrollable stimuli can effect measurement (viral infection, circadian rhythm)
Leukocyte Telomere Length	- Consistent with population analysis	- Inconsistent for individual analysis - Uncontrollable factors stimuli can effect measurement (G-CSF) - Lengthy process
***p16^{INK4a}* mRNA in T-lympocytes**	- Straightforward assay - Consistent with both population and individual analysis	- SNPs at locus can affect expression - Controllable stimuli can effect measurement (smoking, exercise) - Lengthy process

Table 1: Summary of the strengths and weaknesses of aging biomarkers

CHAPTER 2: GERONTOGEN TESTING IN *p16*^{LUC} REPORTER MICE

2.1 Introduction

Murine models have played a critical role in the identification and classification of carcinogens. For example, commercially available animal models, (*i.e.* BigBlue^{TM}, MutaMouse^{TM} and the *p53*$^{+/-}$ strain) (Goldsworthy et al., 1994; Jacobson-Kram et al., 2004; Long et al., 2010), comprise core tools in cancer toxicological assessment. These reagents have enhanced our basic understanding of carcinogenesis, and have contributed to public health by increasing the efficiency and sensitivity of carcinogen identification while reducing animal requirements and research costs. In 1987, George Martin proposed the concept of "gerontogens" (Martin, 1987); that is, environmental agents which accelerate molecular aging analogous to the way carcinogens accelerate neoplasia. While murine models for carcinogen testing are advanced, *in vivo* tools for gerontogen testing do not exist.

Mammalian aging is complex, with several distinct molecular processes contributing to age-related tissue dysfunction and morbidity. While no single molecular process underpins all aspects of mammalian aging, several lines of evidence suggest the activation of senescence is an important contributor to aging. Markers of cellular senescence dramatically increase with aging in humans and mice, including expression of the *p16*^{INK4a} tumor suppressor gene (Krishnamurthy et al., 2004; Liu et al., 2009; Nielsen et al., 1999; Zindy et

al., 1997). Moreover, activation of *p16*^{INK4a} and senescence has been linked to replicative hypofunction in several tissues (*i.e*. neural stem cells (Molofsky et al., 2006), hematopoietic progenitors (Janzen et al., 2006), lymphocytes (Liu et al., 2011; Signer et al., 2008), and pancreatic beta-cells (Krishnamurthy et al., 2006)). Altered regulation of the senescence promoting *CDKN2a/b* locus, which encodes p16^{INK4a}, p15^{INK4b} and ARF, has been linked to age-associated phenotypes including atherosclerotic disease, type II diabetes, glaucoma and several malignancies (Jeck et al., 2012). Finally, pharmacologic and genetic approaches to manipulate the number of senescent cells *in vivo* can ameliorate age-associated phenotypes such as sarcopenia, kyphosis, and hypo-replication of T-lymphocytes and pancreatic beta-cells (Baker et al., 2011; Berent-Maoz et al., 2012; Chen et al., 2011a). Given these intimate links between aging, *p16*^{INK4a} expression, and senescence induction, we sought to determine if *in vivo* activation of *p16*^{INK4a}, measured through the use of a recently described reporter allele (Burd et al., 2013), could be used to assess the gerontogenic effects of environmental agents.

2.2 Materials and Methods

Experiments were performed under protocols approved by the institutional care and use committee (IACUC) of the University of North Carolina. Hairless SKH1-E *p16*$^{LUC/+}$ mice were used for all experiments.(Burd et al., 2013) Genotyping was performed as previously described.(Burd et al., 2013) For histologic analysis, tissues were fixed with 10% formalin overnight, and then transferred to 70% ethanol for paraffin blocking and staining. All slides were generated and stained with Hematoxylin and Eosin at the UNC

Histopathology Core. Quantitative TaqMan RT-PCR strategies for the detection of *p16*^{INK4a} were performed as previously described (Krishnamurthy et al., 2006; Krishnamurthy et al., 2004). Statistical significance was determined using a student's t-test or linear regression analysis for all comparisons except survival analysis, where the Gehan-Breslow-Wilcoxon test was employed.

2.2.1 Exposures

High Fat Diet: 42% Fat diet (HFD) was ordered from Harlan Laboratories (TD.88137). At 8-10 weeks of age, mouse chow was changed to HFD vs. normal diet (4% fat) after initial baseline imaging. New diet was refilled once a week. Twenty male and female SKH1-E *p16*$^{+/LUC}$ mice were analyzed per dietary cohort (42% vs. 4%) for 84 weeks.

Hepatic Steatosis Evaluation: Livers were incubated in 4% Osmium overnight, washed with diH_2O, and then fixed with 10% Formalin. Tissues were then imbedded, sectioned and stained with Hematoxilyn and Eosin using the Immunohistochemistry core facility.

Data Analysis: Linear regression analysis was completed to determine the relationship between p16^{LUC} signal and weight in HFC cohort at 52 weeks of exposure.

Arsenic: Sodium arsenite (As) was ordered from Sigma (71287-250G) and dissolved in sterile water at 50 ppm. At 10-12 weeks of age, mouse water was changed to 50 ppm vs. 0 ppm arsenic after initial baseline imaging. New water was refilled once a week. Twenty male and female SKH1-E *p16*$^{+/LUC}$ mice were analyzed per arsenic cohort (50 ppm vs. 0 ppm) for 48 weeks.

Pancreatic Islet Measurements: Randomized 10x histological images were taken of the pancreas in each cohort. Each islet was then carefully traced and the area was measured using imageJ analysis.

Cigarette Smoke: Cigarettes were ordered from the University of Kentucky (3R4F)—through the Reference Cigarette Program at College of Agriculture in Lexington, Kentucky. Beginning at age 10-12 weeks after baseline imaging, mice were exposed to one hour of cigarette smoke/day, five days/week. For exposure, mice were put into an inExpose exposure system providing both mainstream and side stream smoke exposure. Control animals (no smoking exposure) were handled in an identical manner except were not exposed to tobacco smoke. Ten male SKH1-E $p16^{+/LUC}$ mice were analyzed per tobacco cohort (smoking vs. non-smoking). Animals were exposed to tobacco smoke for 24 weeks, but were imaged for an additional 32 weeks after exposure.

UV light: A UVB lamp from UVP was used for these studies, with an emission spectrum of 290-350 nm light, and with a peak emission at 312 nm. At 8-10 weeks of age, mice were exposed to 353 J/m^3 of UVB light three times per week for 24 weeks. UV exposure began after initial baseline imaging. Fifteen male SKH1-E $p16^{+/LUC}$ mice were analyzed per UVB cohort (exposed vs. unexposed) for 16 more weeks after exposure. UV exposed mice were sacrificed for morbidity or tumor burden in accordance with established laboratory protocols.

Phospho-Histone H2A.X Immunohistochemistry: Skin tissues were incubated overnight with 1/500 of Phospho-Histone H2A.X (Ser139) (20E3) Rabbit mAb (Cell Signaling Cat # 9718) according to Cell Signaling standard immunohistochemistry instructions.

Data analysis: All H2AX cells in the epithelial layer of the exposed skin were divided by the total number of epithelial cells in the microscopic field. Fisher's exact test was used to determine statistical significance.

Senescence-Associated ß-galactosidase (SA-ß-gal) activity: Skin was assayed using Cellular Senescence Assay Kit (KAA002; Millipore, USA) according to manufacturer's instructions.

2.2.2 *In vivo* Luminescence Imaging

Luciferase Imaging: To serially monitor luciferase induction, mice were imaged as previously described (Burd et al., 2013) using a Xenogen IVIS LUMINA/KINETIC Imaging System. Imaging was completed under anesthesia, immediately after D-luciferin injection (10 mg/ml in sterile PBS). Sequential imaging was used to determine optimal luminescence. A sequence of 2 min, 2 min, 2 min, 2 min, 30 sec, and 1 min were used. The 4^{th} two minute image (8 minutes after initial injection) was used for all reported imaging measurements. For arsenic, high fat diet, and cigarette smoke exposure images were taken of the ventral side of the mouse. For UV light, the dorsal (exposed) and ventral (unexposed) sides of each mouse were taken. Living Image 3.1 Software (Caliper Life Sciences) was used to analyze the images at the same image exposure time point (8 min) over the life span of the mouse. Representative images are shown with exposed and unexposed animals for each cohort, as well as appropriate imaging scales to account for imaging settings.

Data Analysis: The raw average radiance values (photon/sec/cm^2/steradian) from the original images were used. A wide angle lens (FOV-24) was used to capture images of 3 or more mice. For each exposure, mice were imaged at least every other month for up to one year,

although some animals were imaged more frequently during the initial stages of each exposure period. Each mouse was circled to measure average radiance values (p/s/cm^2/sr) over the region of interest. The area for each mouse was held constant for each experiment. A blank area on the image was also circled to allow for subtraction of background noise. To omit background noise from each individual mouse image, the background circle was subtracted from the mouse circle. To graph the luciferase induction over time, all murine luciferase signals in a specific cohort were averaged at time zero and normalized to a value of one. All subsequent mouse images were then normalized relative to the average time zero luminescence.

2.3 Results

The *p16^{LUC}* allele features firefly luciferase 'knocked-in' to exon 1α of the murine *Cdkn2a* locus, which includes the *p16^{INK4a}* transcriptional start site (Burd et al., 2013). This allele places luciferase under the control of the endogenous *p16^{INK4a}* promoter as well as cis-regulatory elements, which are known to extend for several hundred kilobases around the locus (Burd et al., 2010; Visel et al., 2010). Importantly, expression of *p16^{INK4a}* is negligible in healthy cells from young mice, but accumulates with age-promoting stresses, and subsequent senescence. Additionally, cellular expression of *p16^{INK4a}* increases more than 300-fold on a per cell basis (Burd et al., 2013; Krishnamurthy et al., 2004). This large, dynamic range of *p16^{INK4a}* expression makes *p16^{LUC}* a valuable tool for *in vivo* imaging of senescence induction. To assess the impact of candidate gerontogens (*i.e.* high fat diet, UV

light, arsenic, and cigarette smoke) on senescence, we performed serial analysis of $p16^{LUC}$ cohorts. Hairless SKH1-E mice were used for all studies to further enhance *in vivo* imaging.

2.3.1 High Fat Diet

Prior studies on the effects of obesity and high fat diet (HFD) on $p16^{INK4a}$ expression *in vivo* have yielded inconsistent results. For example, HFD has been reported to increase senescence and/or $p16^{INK4a}$ expression in the murine or baboon vascular cells (Shi et al., 2007; Wang et al., 2009), whereas $p16^{INK4a}$ mRNA expression in peripheral blood T-lymphocytes (PBTL) does not correlate with body-mass index, a marker of obesity, in humans (Liu et al., 2009). To explicitly examine the effects of high fat diet on whole body senescence *in vivo*, littermate $p16^{LUC}$ mice were placed on a 42% (HFD) or 4% fat diet (normal diet, ND) for 18 months starting at 8-10 weeks of age. HFD produced a clear pharmacodynamic effect, causing significant weight gain (Supplemental Figure 2.1A) and hepatic steatosis (Supplemental Figure 2.1B). Overall survival was not significantly different between the HFD and ND cohorts (Supplemental Figure 2.1C). Consistent with prior reports (Burd et al., 2013; Krishnamurthy et al., 2004), we observed an exponential increase in $p16^{INK4a}$ expression with aging, however the rate of increase in $p16^{INK4a}$ expression assessed by total body luciferase imaging (TBLI) was not different for animals fed on a HFD versus ND (Figures 2.1, A and B). Due to the wide range of weight gain among the mice on HFD, we analyzed the relationship between weight and luciferase intensity at 52 weeks and observed no correlation (Supplementary Figure 2.1D). Correspondingly, expression of $p16^{INK4a}$ mRNA was not altered in liver and spleen harvested from 18-month old mice fed HFD versus ND (Supplementary Figure 2.1E). These data suggest that HFD does not

accelerate the accumulation of senescent cells *in vivo,* at least to the level of sensitivity of luciferase detection.

2.3.2 Arsenic

Arsenic is a common environmental toxicant that has been linked to phenotypes associated with human aging (*i.e.* several cancers, type II diabetes and atherosclerosis) (Kapaj et al., 2006). While not a direct clastogen, arsenic induces oxidative genotoxicity, and may decrease DNA repair (Andrew et al., 2003; Hartwig et al., 1997; Yamauchi et al., 2004). We examined the effect of chronic arsenic exposure on $p16^{INK4a}$ expression *in vivo.* For this experiment, littermate $p16^{LUC}$ mice were given 50 ppm arsenic or 0 ppm arsenic in the drinking water for 12 months starting at 8-10 weeks of age. After 48 weeks of exposure, mice on 50 ppm arsenic had an average of 1.5 ppm arsenic accumulation in the liver as measured by mass spectrometry (Supplemental Figure 2.2A). Consistent with the known effects of arsenic (Paul et al., 2007), mice on 50 ppm exhibited small, structurally deranged pancreatic islets (Supplemental Figure 2.2, B and C) with an extreme decrease in total islet mass (Supplemental Figure 2.2C), but overall survival rates were not altered with arsenic exposure (Supplementary Figure 2.2D). Additionally, the exocrine portion of pancreas appeared normal in the exposed animals. A modest, but significant increase in $p16^{INK4a}$ expression was observed by 24 weeks of exposure using TBLI (Figure 2.2, C and D) ($p=0.023$). In accord with the TBLI results, expression of $p16^{INK4a}$ mRNA was higher in spleen but not liver of one year old mice on 50 ppm versus 0 ppm arsenic (Supplemental Figure 2.2E). These data suggest that chronic arsenic exposure modestly accelerates the accumulation of senescent cells *in vivo*.

2.3.3 Cigarette Smoke

Research shows that mutagens in cigarette smoke promote DNA damage (DeMarini, 2004; Pfeifer et al., 2002) and smoking promotes age-related diseases such as emphysema, atherosclerosis and several cancers (Bernhard et al., 2007; Ito and Barnes, 2009). Chronic cigarette smoke exposure in humans is associated with an increased $p16^{INK4a}$ expression in PBTL (Liu et al., 2009; Nelson et al., 2012). To determine the effects of moderate dose tobacco smoke exposure on cellular senescence *in vivo*, littermate $p16^{LUC}$ mice were exposed to cigarette smoke (CS) or ambient air (AA) for one hour per day, five days per week for six months starting at 10-12 weeks of age. After six months of exposure, mice were aged without cigarette smoke for up to one year. At the end of the one year study, histological analysis of the sinus cavity of CS mice showed particulate deposits along the epithelial layer of the nasal papilla in exposed animals, whereas no differences were noted in lung architecture between CS and AA cohorts at this tobacco dose (Figure 2.2A). Additionally, this moderate tobacco dose was not associated with increased mortality (Supplemental Figure 2.3A). There was a significant increase in $p16^{INK4a}$ accumulation between the CS and AA cohorts as measured by TBLI which was readily noted within weeks of CS exposure, and persisted even after CS exposure was discontinued (Figure 2.2B). Consistent with histologic examinations of the nasal cavities and lungs (Figure 2.2A), specific luciferase induction was noted in the head and neck region of mice, but not the thoracic and abdominal regions (Figure 2.2C). Correspondingly, $p16^{INK4a}$ mRNA levels in the liver, lung, axillary lymph nodes and spleen were similar in one year old CS and AA mice (Supplemental Figure 2.3B). These data suggest that low-dose, chronic CS exposure accelerates the accumulation of senescent cells in the tissues (*i.e.* nasal epithelium) that receive the highest exposure.

2.3.4 UV Light

Chronic UVB exposure causes photoaging and skin cancer (Kligman, 1989; Scharffetter-Kochanek et al., 2000). Prior work has suggested that acute UVB exposure can rapidly induce $p16^{INK4a}$ expression in human skin (Pavey et al., 1999). To directly assess the effects of chronic UVB on the induction of senescence *in vivo*, the dorsal surface of $p16^{LUC}$ mice were exposed to 350 J/m^2 of UVB light three times a week for six months starting at 10-12 weeks of age. Littermate control mice were contemporaneously aged in the absence of UVB. After six months of exposure, mice were aged without further UVB exposure until they reached one year of age. After six months of exposure, mice exposed to chronic UV light had more epidermal hyperkeratosis and metaplasia than the non-exposed cohort (Figure 2.3A, upper panel). The UV-exposed cohort exhibited more inflammatory infiltration into the reticular dermis and hypodermis of lymphocytes and neutrophils than non-exposed controls (Figure 2.3A, middle panel). A marker of DNA damage, phospho-H2AX staining, was significantly increased in the epithelial layer of skin in UV exposed mice than non-exposed mice, suggesting a persistent DNA damage response (Figure 2.3A, lower panel, and Supplemental Figure 2.4A). Additionally, UVB exposed mice developed skin neoplasms starting five months into the window of exposure (Figure 2.3B) which were associated with increased mortality (Figure 2.3C). Accumulation of luciferase was higher in $p16^{LUC}$ animals treated with UV than unexposed controls prior to development of visible neoplasms and TBLI was almost ~8 times greater in UV-treated animals after 32 weeks of exposure (Figure 2.3D). In accord with the TBLI results (Figure 2.3E), $p16^{INK4a}$ mRNA levels from abdominal and dorsal skin of one year old mice from both cohorts confirmed the site-specific induction

of 16^{INK4a} expression (Figure 2.3F). Additionally, the UV exposed dorsal skin exhibited higher expression than unexposed abdominal skin from the same mouse (Figure 2.3F).

To confirm the induction of senescence *in vivo* using additional markers, we analyzed exposed and unexposed skin tissue for senescent associated (SA) cytokines, *CXCL-1* and *IL-6*, as well as SA-β-galactosidase staining (SA-β-gal). Expression of *CXCL-1* and IL-*6* increased in mice exposed to UV light when compared to non-exposed control mice. Additionally, the increase of these mRNAs only occurred in skin that was directly exposed to UV light (back) when compared to non-exposed skin (abdomen) of the same animals (Figure 2.3, G and H). Lastly, we observed a similar pattern of SA-β-gal staining. Increased staining was observed in the skin from the back but not abdomen of the UV-treated mice (Supplemental Figure 2.4B). These data suggest that chronic DNA damage from UV light accelerated the accumulation of senescent cells *in vivo*.

2.4 Discussion

In this work, we demonstrate that serial imaging of $p16^{LUC}$ mice can be used to study the senescence-promoting effects of environmental exposures such as arsenic, HFD, CS, and UVB. Through this approach, we found evidence that direct DNA damaging agents (*i.e.* CS and UV light) are potently gerontogenic with a lesser, but significant, effect of chronic arsenic exposure. Moreover, using this *in vivo* reporter system, we identified the anatomic effects of these agents with regard to molecular aging. For example, we showed the most marked effects of CS administered at modest dose by passive inhalation are on nasal epithelia

as opposed to lung parenchyma (Figure 2.2C) and that the most marked effects of UVB are on exposed rather than unexposed skin (Figure 2.3, E and F).

It is important to note two limitations of this system. First, while luciferase imaging is considerably more sensitive than optical methods, the $p16^{LUC}$ allele may be less useful for the detection of senescence induction in deeper organs or in rare cellular subtypes. Therefore, while we observed no effect of HFD on $p16^{INK4a}$ induction at the total-body imaging level, it is possible HFD activates senescence in important cellular compartments (e.g. pancreatic beta-cells (Sone and Kagawa, 2005), and vascular cells (Shi et al., 2007; Wang et al., 2009)), but not to a level detectable using this system. Secondly, activation of $p16^{INK4a}$ expression is only one component of molecular aging, which is a complex and multi-faceted process. Therefore, the $p16^{LUC}$ system does not detect cellular aging processes that occur independently of $p16^{INK4a}$ expression; and likewise cannot be used to identify $p16^{INK4a}$-independent gerontogens.

In summary, we have shown that the $p16^{LUC}$ allele faithfully reports the *in vivo* activation of senescence markers in response to environmental toxicants, allowing for the determination of an agent's gerontogenic effects using modest-sized cohorts of serially analyzed animals. We believe this resource can supplement other rodent platforms used for toxicological assessments; in particular, providing an *in vivo* system to assess a compound's age-promoting activity. Finally, we believe this system will enhance our understanding of basic aging biology, by providing a tractable system for serial pharmacologic studies of aging in mice.

2.5 Figures

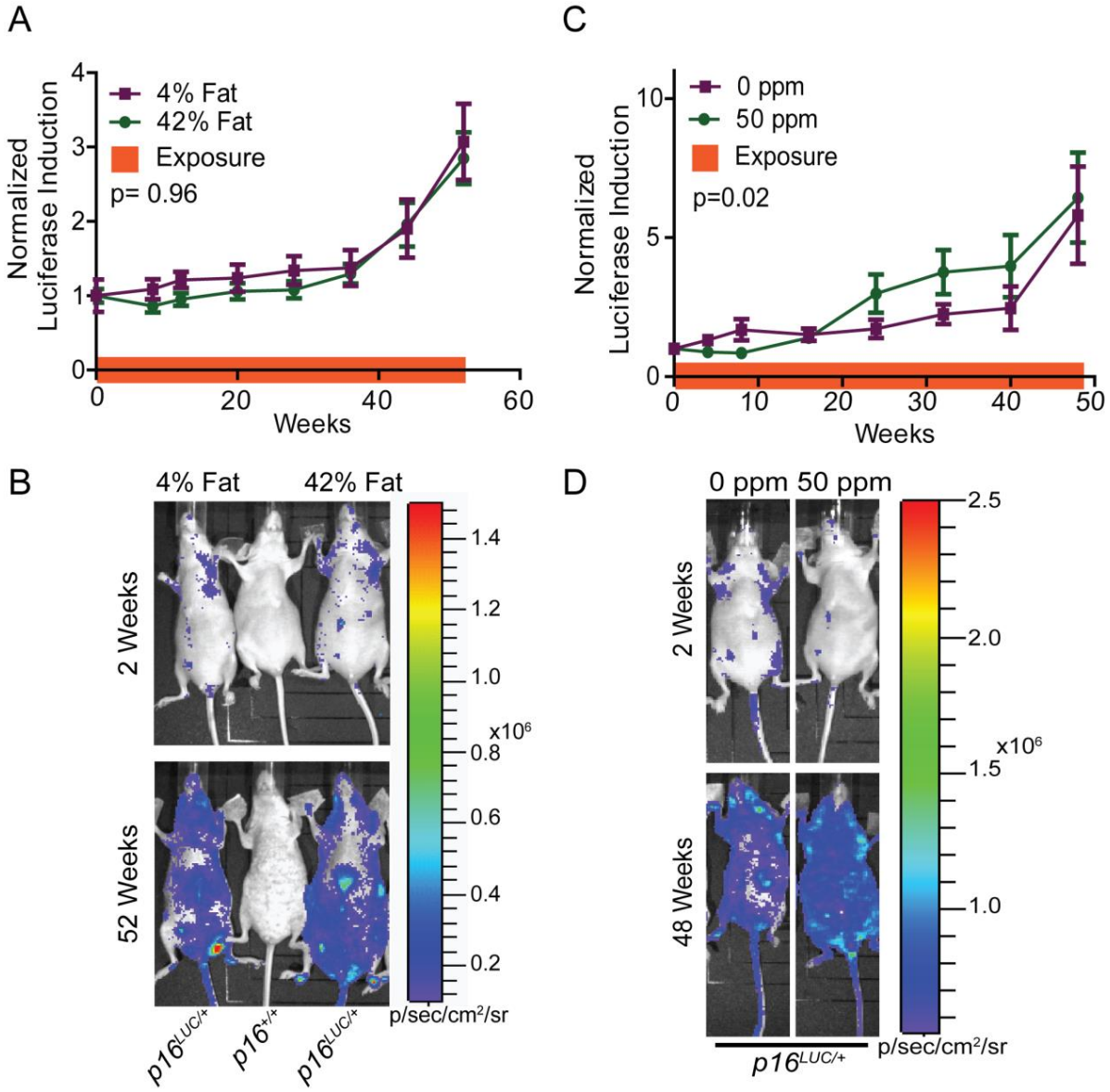

Figure 1 (Sorrentino)

Figure 2.1: High fat diet does not increase *p16*^{INK4a} expression, while arsenic moderately increases *p16*^{INK4a} expression in p*16*^{LUC} mice.

(A) Luciferase levels were measured periodically *p16*^{LUC} mice fed a high fat diet (green) or a normal diet (purple) as measured by total body luciferase radiance (TBLI). Luciferase levels were normalized to the mean luciferase levels of the entire cohort at day 0 and graphed as a

function of time. The orange bar on x-axis indicates duration of exposure. Error bars indicate standard error of the mean. P values were determined through linear regression analysis. (B) Representative images (52 weeks) of the study described in 'A' are shown. (C) Luciferase levels were measured periodically $p16^{LUC}$ mice exposed to 50 ppm arsenic (green) or 0 ppm (purple) as measured by TBLI (50 ppm, n=23, 0 ppm, n=14). Results were recorded, analyzed, and displayed as in Figure 1A. (D) Representative images (48 weeks) of the study described in 'C' are shown.

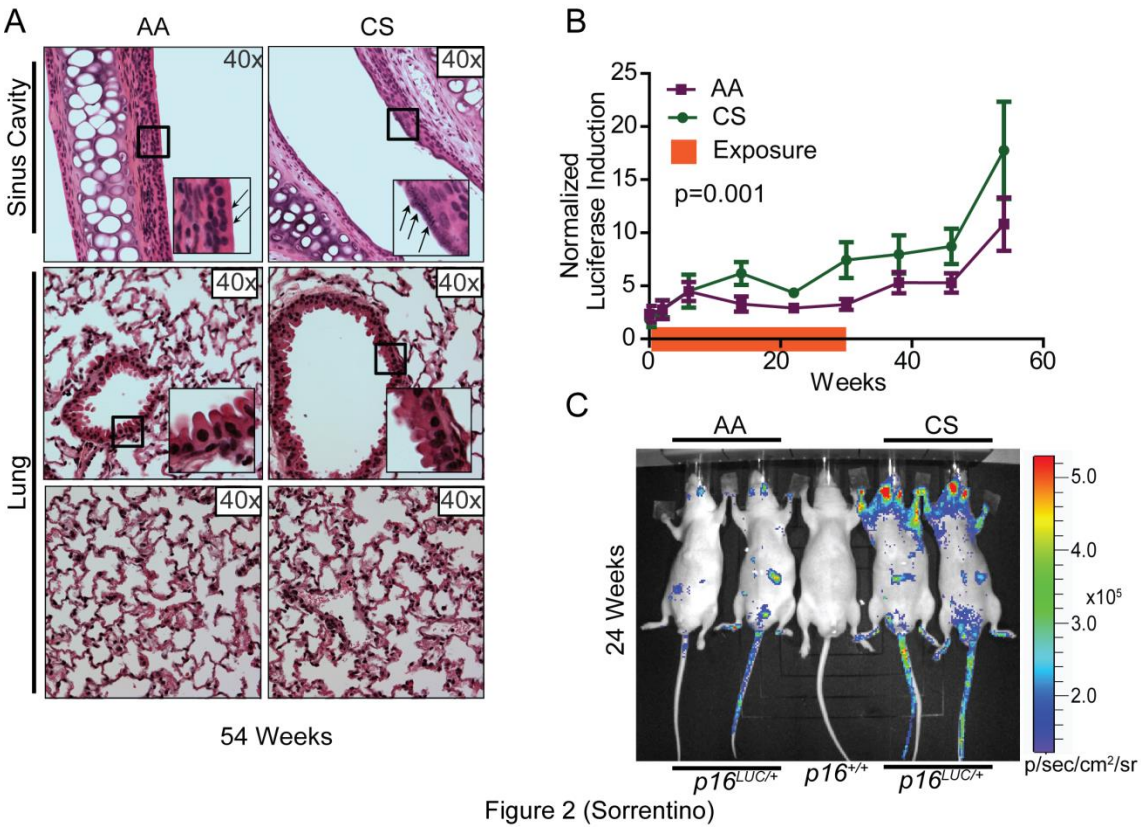

Figure 2 (Sorrentino)

Figure 2.2: Cigarette smoke increases *p16*^{INK4a} expression in p*16*^{LUC} mice.

(A) Representative histological images of the upper sinus cavity (upper panel), airway bronchioles (middle panel), airway epithelium peg cells highlighted), and alveolar sacs (lower panel) from CS and AA mice after 54 weeks of exposure were stained with Hematoxylin & Eosin (H&E). (B) Luciferase levels were measured periodically in *p16*^{LUC} mice exposed to cigarette smoke (green) or ambient air (purple) (CS, n=10; AA, n=10). Results were recorded, analyzed, and displayed as in Figure 1A. (C) Representative images (24 weeks) of the experiments described in 'B' are shown.

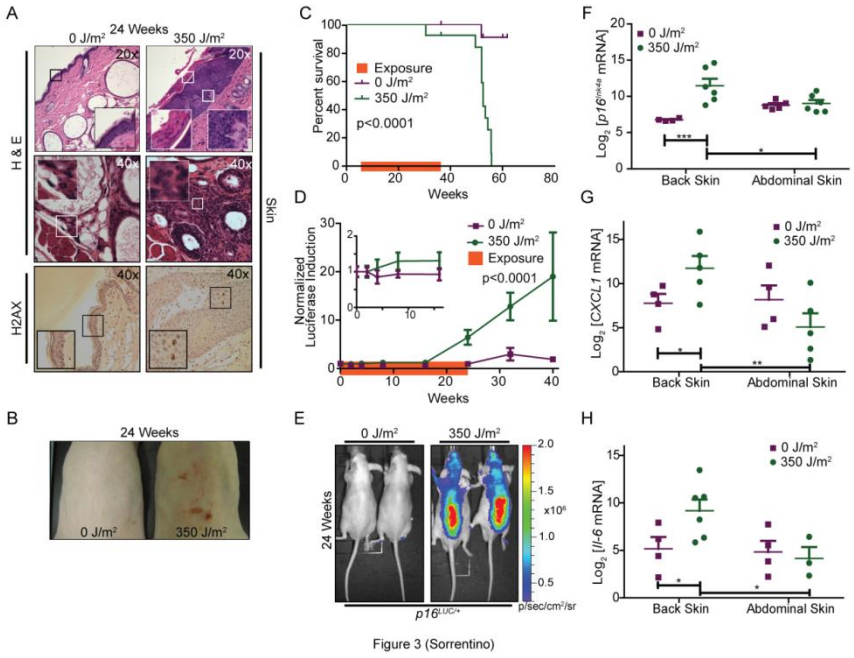

Figure 2.3: UVB light increases *p16*^{INK4a} expression in p*16*^{LUC} mice.

(A) Representative histopathological images of skin exposed (left) and not exposed (right) to UV light at sacrifice stained with H&E (top, middle) or phospho-H2AX (lower). Both sections show dilated sebaceous glands and small, deranged hair papillae which is normal for these hairless mice. (B) Representative dorsal images of mice (UV vs. non-exposed) after 6 months of exposure. (C) Kaplan-Meier curve of mortality in the CS and AA cohorts ($p<0.0001$). (D) Luciferase levels were measured periodically in *p16*^{LUC} mice exposed to 350 J/m^2 (green) or 0 J/m^2 (purple) with emphasis on initial 20 weeks of exposure (inset) (350 J/m^2, n=13; 350 J/m^2, n=11). Results were recorded, analyzed, and displayed as in Figure 1A. (E) Representative images (24 weeks) of the experiments described in 'D' are shown. (F) Quantitative realtime PCR of *p16*^{INK4a} expression in the back and abdominal skin of UV treated and untreated mice at sacrifice. *$p<0.05$, **$p<0.01$, ***$p>0.005$.

2.6 Supplemental Figures

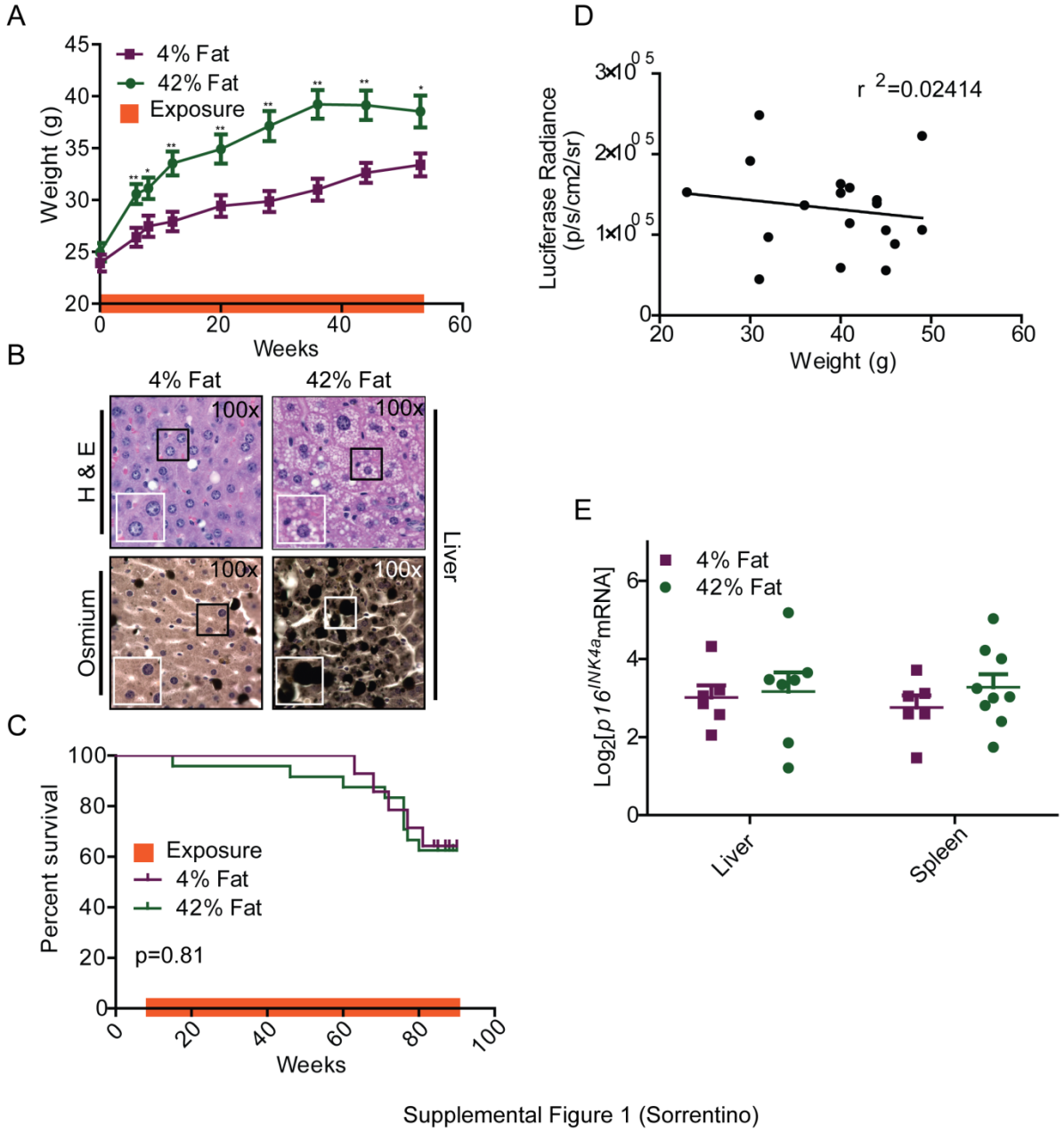

Supplemental Figure 1 (Sorrentino)

Supplemental Figure 2.1: Physiologically effective doses of high fat diet do not affect the survival rates of mice, and quantitative realtime PCR validates *p16*^{INK4a} expression as measured by TBLI.

(A) The body mass of mice fed a high fat (HFD; 42% fat) or normal (ND; 4% fat) diet during the 52-week period of exposure (orange bar) (HFD, n=24; ND, n=15). *$p<0.05$, **$p<0.01$. (B) Representative histopathological images of hemotoxylin and eosin (top) and osmium tetroxide (bottom) stained liver tissue from HFD mice ND mice at 84 weeks of exposure. Hepatocytic lipid droplets are stained black and indicate severe steatosis in the high fat chow liver (right). (C) Kaplan-Meier curve of mortality in the HFD and ND cohorts ($p=0.8078$) (D) Graph measuring individual weight vs luciferase induction ($r^2=0.024$). (E) Quantitative realtime PCR analysis of $p16^{INK4a}$ expression in livers and spleens of each cohort at the after 84 weeks of exposure. Orange bar on x-axis indicates duration of exposure. Error bars indicate standard error of the mean.

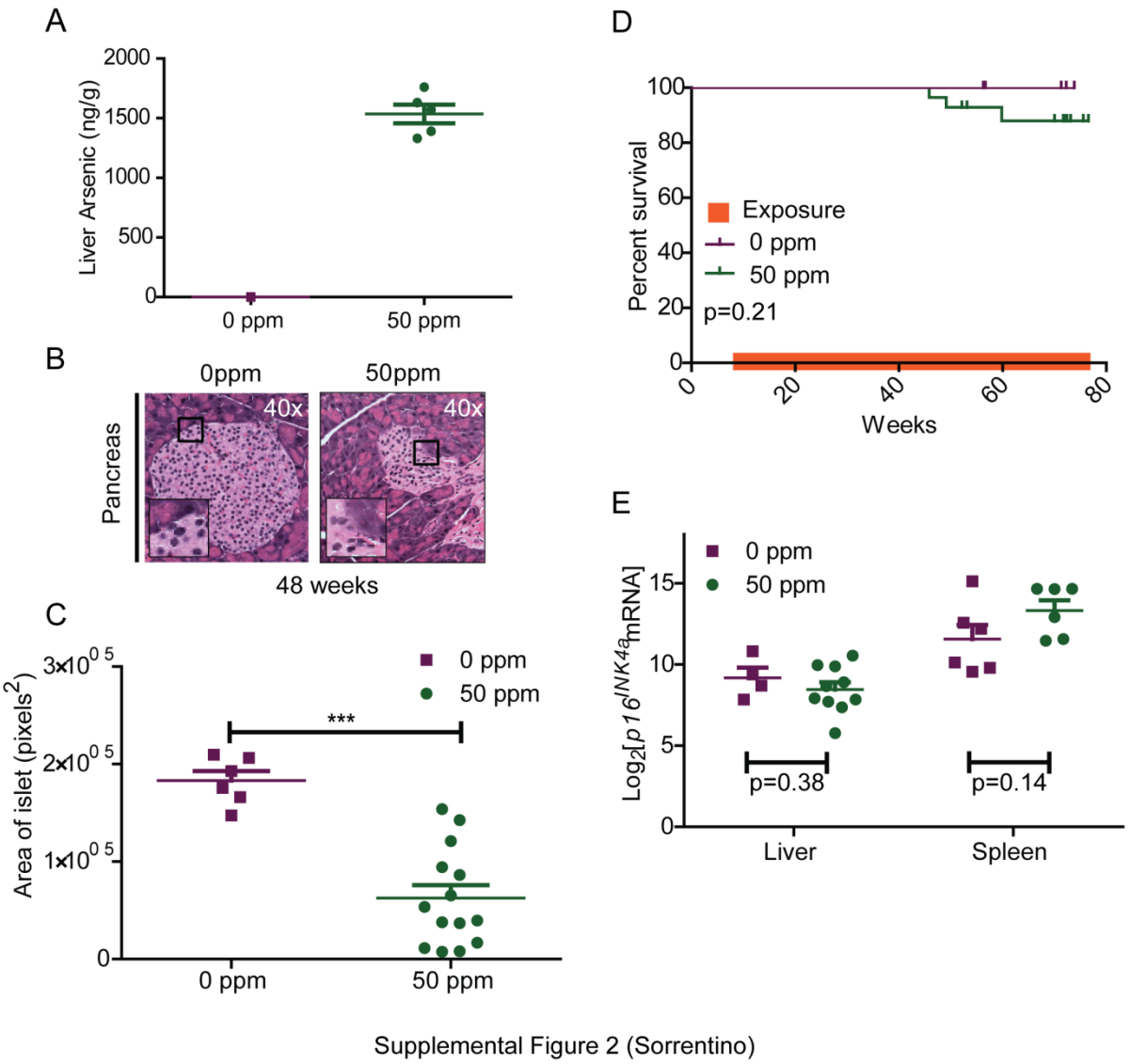

Supplemental Figure 2 (Sorrentino)

Supplemental Figure 2.2: Physiologically effective doses of arsenic do not affect the survival rates of mice, and quantitative realtime PCR validates *p16^{INK4a}* expression as measured by TBLI.

(A) Level of arsenic (ng/g) found by mass spectrometry in the liver of mice treated with 50 ppm or 0 ppm arsenic for 48 weeks. (B) Representative hematoxylin and eosin stained sections of the pancreas 48 weeks following exposure to 0 ppm or 50 ppm arsenic. (C) Area of individual islets in the pancreas of mice exposed to 0 ppm or 50 ppm arsenic. (D) Kaplan-

Meier curve of mortality in the 50 ppm and 0 ppm cohorts (p=0.5164). (E) Quantitative realtime PCR of *p16*^{INK4a} in the liver and spleen in 50 ppm and 0 ppm mice after 52 weeks of exposure. Orange bar on x-axis indicates duration of exposure. Error bars indicate standard error of the mean. ***p<0.0001

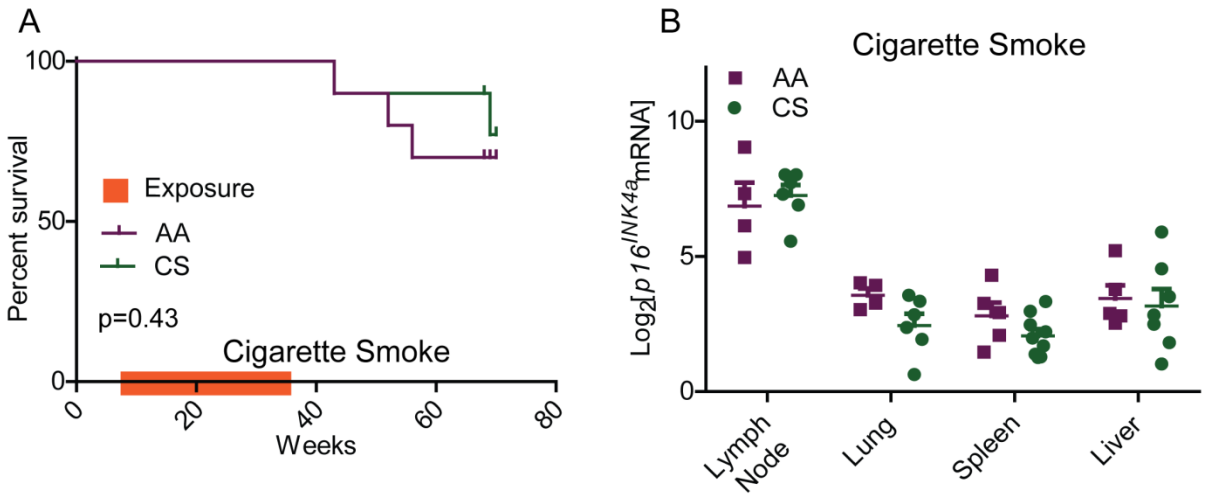

Supplemental Figure 3 (Sorrentino)

Supplemental Figure 3: Cigarette smoke does not affect the survival rates of mice, and quantitative realtime PCR validates *p16*^{INK4a} expression as measured by TBLI

(A) Kaplan-Meier curve of mortality in the CS and AA cohorts (p=0. 4361). (B) Quantitative realtime PCR of *p16*^{INK4a} expression in the livers, spleens, lungs and lymph nodes of CS and AA mice after 52 weeks of exposure. Orange bar on x-axis indicates duration of exposure. Error bars indicate standard error of the mean. ***p<0.0001

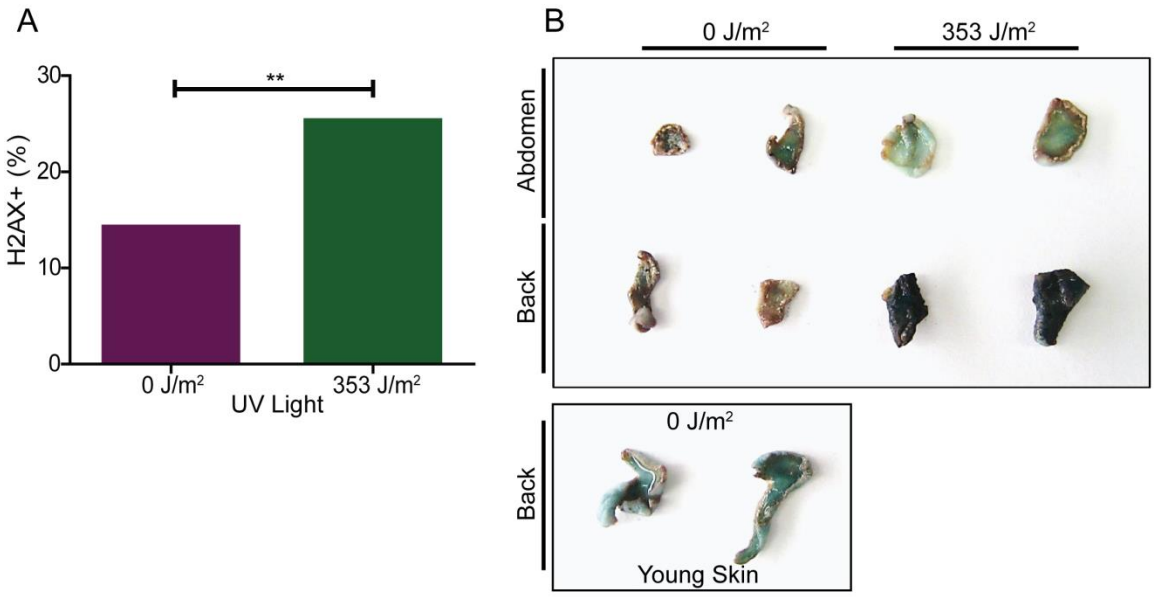

Supplemental Figure 4 (Sorrentino)

Supplemental Figure 2.4: UV light leads to a senescent phenotype in skin.

(A) Quantitative analysis of H2AX staining in the back skin of UV exposed and non-exposed cohorts. (B) SA β-galactosidase staining of skin from the backs and abdomens of UV exposed and unexposed mice. Unexposed back skin from young mice (8 weeks old) was used to determine background staining (bottom). **$p<0.01$

CHAPTER 3: REGULATION OF TRANSIENT INDUCTION OF $p16^{INK4a}$

3.1 Introduction

The cell cycle inhibitor, $p16^{INK4a}$, has been well documented as a tumor suppressor protein that once transcriptionally activated, will lead to cellular senescence, a permanent state of growth arrest. Additionally, prior work has shown that there is accumulation of senescent cells in aging tissue (Krishnamurthy et al., 2004; Liu et al., 2009; Serrano et al., 1997). However, there has been limited work to describe the transient induction of $p16^{INK4a}$ expression *in vitro* and even less *in vivo*. A few groups have described genetic manipulation of $p16^{INK4a}$ using inducible constructs to cause temporary increase in expression leading to a growth pause, instead of senescence *in vitro* (Frost et al., 1999; Rossi et al., 1998; Stone et al., 1996). Using cell lines, one group showed that $p16^{INK4a}$ expression for 1 day arrested the cells in G1. However, upon return to $p16^{INK4a}$ baseline levels, the cells resume growth after 3-5 days. Interestingly, if $p16^{INK4a}$ was induced for 6 days, the cells never again proliferated and developed a senescent phenotype (Dai and Enders, 2000), suggesting a temporal trigger to transition the cell from a G1 pause to permanent growth arrest. While *in vitro* work is helpful, the questions understanding transient induction of $p16^{INK4a}$ *in vivo* remain unanswered.

Research has shown that there is an induction of *p16*^{INK4a} at the site of wound closure in both cells and humans. More specifically, others have shown that induction of matricellular protein, CCN1, will cause *p16*^{INK4a}-dependent fibroblast senescence at site of wound repair and inhibit fibrosis during tissue repair (Jun and Lau, 2010a, b). Additionally, p16^{INK4a} has been associated with keratinocyte migration during wound repair. Laminin5, a basement membrane protein, is co-expressed with p16^{INK4a} along the edges of a wound in culture and *in vivo* (Natarajan et al., 2005; Natarajan et al., 2003). Additionally, during migration, *p16*^{INK4a} is induced to lessen the potential for invasion and transformation (Natarajan et al., 2006). Chronic wound healing has been shown to cause squamous cell carcinoma with loss of known senescence markers including *p16*^{INK4a} and *MMP-19* (Impola et al., 2005; Telgenhoff and Shroot, 2005).

UV burn repair has a very similar physiology to wound regeneration. Both insults lead to a re-epithelialization, inflammatory repsonse, and formation of granulation tissue (Singer and Clark, 1999). Exposure to high doses of UV light has also been shown to cause induction of *p16*^{INK4a} leading to cell cycle arrest in Hela cells (Wang et al., 1996). Additionally, many groups have shown that chronological aging, which has a strong correlation with *p16*^{INK4a} expression in both mice and humans (Krishnamurthy et al., 2004; Liu et al., 2009; Nelson et al., 2012; Zindy et al., 1997), will lead to a slower healing response, including delayed re-epithelialization, delayed angiogenesis, and decreased secretion of growth factors, after exposure to high doses UV light (Gilchrest et al., 1982; Gosain and DiPietro, 2004). Others have also shown that the components of Retinoblastoma (Rb) pathway, which includes *p16*^{INK4a}, are important targets of UV-induced mutagenesis during melanoma development (Kannan et al., 2003). Given these intimate links between

wound healing, UV light and *p16*^{INK4a} expression, we sought to determine the magnitude and duration of transient *p16*^{INK4a} activation upon insult, measured through the use of a recently described reporter allele *in vivo*.

During tissue repair, macrophages have been shown to infiltrate the wound site to clear remaining pathogens and cellular debris by day 4 (DiPietro, 1995). Once activated, macrophages will signal neighboring cells for excretion of growth factors and cytokines to help regenerate the damaged tissue (Martin, 1997). Research has also shown age-related differences in MCP-1 production, a monocyte chemoattractant protein, to the wound following burn injury *in vivo*. More specifically, the levels of MCP-1 in aged burned mice were less than half the levels of young burned mice 1 day after burn, suggesting an association between *p16*^{INK4a} expression and monocyte chemoattractant production (Shallo et al., 2003). Lastly, the *CDKN2A* locus, which encodes *p16*^{INK4a} and *ARF* transcripts, is associated with macrophage proliferation and recruitment during atherosclerotic (an age-related disease) development in humans (Kuo et al., 2011). Moreover, *p16*$^{-/-}$ bone marrow-derived macrophages (BMDMs) exhibit a decreased response to classically polarizing IFNγ and LPS, and an increased sensitivity to alternative polarization by IL-4, suggesting a potential role for p16^{INK4a} as a modulator for macrophage activation and polarization (Cudejko et al., 2011). Due to the strong association between *p16*^{INK4a} and macrophage recruitment, we examined the role of macrophages during transient induction of *p16*^{INK4a} through *in vivo* analysis.

3.2 Materials and Methods

Experiments were performed under protocols approved by the institutional care and use committee (IACUC) of the University of North Carolina. Hairless SKH1-E *p16*$^{LUC/+}$ mice were used for all experiments (Burd et al., 2013). Genotyping was performed as previously described (Burd et al., 2013). For histologic analysis, tissues were fixed with 10% formalin overnight, and then transferred to 70% ethanol for paraffin blocking and staining. All slides were generated and stained with Hematoxylin and Eosin at the UNC Histopathology Core. Statistical significance was determined using a student's t-test for all comparisons. All gross anatomy photos were taking with 6.0 megapixel Canon SD630.

3.2.1 Transient Inductions

Wound Generation: At 8-10 weeks of age, mouse p16$^{LUC/+}$ (SKH1-E background) or p16$^{+/+}$ and p16$^{-/-}$ (C57/B6 background) were anesthetized with inhaled 2% isofluorane. Once anesthetized and after cleansing the 1 sq cm area with iodine, a sterile 3 mm punch was used to create one full-thickness wound on the dorsal side of each mouse, just below the shoulder blades. SKH1-E mice were imaged for luciferase following a specific schedule (Figure 1A) until the wound healed. C57/B6 mice wounds were measured weekly using a caliper until completely healed.

UV light: A UVB lamp from UVP was used for these studies, with an emission spectrum of 290-350 nm light, and with a peak emission at 312 nm. At 8-10 weeks of age, mice were exposed to 2000 J/m^3 of UVB once. UV exposure was given after initial baseline imaging.

Mice were imaged for luciferase following a specific schedule (Figure 2A) until wound healed.

3.2.2 Drug Treatments

Dexamethasone: Mice were given a daily intraperitoneal injection (I.P.) of dexamethasone (Sigma D4902) at dose of 7 mg/kg diluted in Phosphate Buffered Solution (PBS) for the first 16 days after wounding (Figure 3A).

IKK-β Inhibitor: Mice were given an intraperitoneal injection (I.P.) of compound A (Dr. Al Baldwin's drug) at dose of 10 mg/kg dose diluted in dimethylsulfoxide (DMSO) starting 6 days before wounding and ending 16 after wounding (Figure 3C).

Clodrosome: Mice were given a daily intravenous injection (I.V.) of liposomal clodronate (Encapsula NanoSciences SKU #STLMDK) at dose of 100 uL/per mouse for the three days before the wounding (Figure 4A).

3.2.3 Flow Cytometry

Bone marrow, splenic, and peripheral white blood cells were isolated as previously described (Kiel et al., 2005). Once the cells were isolated, cells were stained with B220-violet (B cell marker), Gr1-APC-Cy7 (granulocyte marker), F4/80-FITC (macrophage marker), and Mac1-PE-Cy7 (monocyte marker). Flow cytometry analysis was completing using Beckman-Coulter (Dako) CyAn ADP machine with the strategy shown in Figure 4B.

Figure 4B is a schematic that describes the gating strategy for F4/80+Mac1+ population identification. First, all cells with proper size and granularity (FS lin, SS lin) were gated for

B220. Then, all B220- cells where gated for Gr1. Lastly, all Gr-1- cells were gated for Mac1 and F4/80. All Mac1+F4/80+ cells were used for analysis.

3.2.4 In vivo Luminescence Imaging

Luciferase Imaging: To serially monitor luciferase induction, mice were imaged as previously described (Burd et al., 2013) using a Zenogen IVIS LUMINA Imaging System. Imaging was completed under anesthesia, immediately after D-luciferin injection (10 mg/ml in sterile PBS). Sequential imaging was used to determine optimal luminescence. A sequence of 2 min, 2 min, 2 min, 2 min, 30 sec, and 1 min were used. The 4^{th} two minute image (8 minutes after initial injection) was used for all reported imaging measurements. For all exposures, images were taken of the dorsal side of the mouse. Living Image 3.1 Software (Caliper Life Sciences) was used to analyze the images at the same image exposure time point (8 min) over the experiment. Representative images are shown with wounded and non-wounded animals for each cohort, as well as appropriate imaging scales to account for imaging settings. For data analyses, the raw average radiance values (photon/sec/cm^2/steradian) from the original images were used. A wide angle lens (FOV-24) was used to capture images of 3 or more mice.

Data Analysis: For each experiment, mice were imaged following a specific schedule (Day 0, 2, 4, 7, 10, 16). Each mouse was circled to measure average radiance values (p/s/cm^2/sr) over the region of interest. The area for each mouse was held constant for each experiment. A blank area on the image was also circled to allow for subtraction of background noise. To omit background noise from each individual mouse image, the background circle on a non-exposed area of the mouse was subtracted from the exposed area circle. To graph the

luciferase induction over time, all murine luciferase signals in a specific cohort were averaged at time zero and normalized to a value of one. All subsequent mouse images were then normalized relative to the average time zero luminescence.

3.3 Results

The *p16-LUC* allele includes firefly luciferase 'knocked-in' to exon 1α of the murine *Cdkn2a* locus, placing luciferase under the control of the endogenous $p16^{INK4a}$ promoter as well as cis-regulatory elements, which are known to extend for several hundred kilobases around the locus (Burd et al., 2010; Burd et al., 2013; Visel et al., 2010). Expression of $p16^{INK4a}$ can potentially increase to more than 300-fold on a per cell basis making $p16^{LUC}$ a valuable tool for *in vivo* imaging of transient induction of $p16^{INK4a}$ (Burd et al., 2013; Krishnamurthy et al., 2004). To assess the kinetics and duration of $p16^{INK4a}$ expression after dermal insult, we performed serial analysis of $p16^{LUC}$ cohorts. Hairless SKH1-E mice were used for all studies to further heighten *in vivo* luciferase signal.

3.3.1 Wound Healing Model

Research has shown that $p16^{INK4a}$ is induced at the edge of a wound during healing *in vitro* (Natarajan et al., 2003). Others have also shown that chronic wounding will lead to $p16^{INK4a}$-associated skin cancers (Telgenhoff and Shroot, 2005). Using the previously characterized $p16^{LUC}$ allele, we sought to determine the duration of $p16^{INK4a}$ during wound regeneration. SKHI-E mice were imaged for a baseline and then immediately wounded on the dorsal side between the shoulder blades. Mice were serially imaged for up to a month

until the wound was healed (Figure 1A). Through observation and histological analysis, wounds healed as previously recorded (Figure 1B) (Bradshaw et al., 2002) . There was clear induction of $p16^{INK4a}$ at the site of the wound by 2 days after wound generation, with peak induction by 4 days (Figure 1, D and E). $p16^{INK4a}$ expression returned to baseline by 16 days, when the wound had healed (Figure 1D). To determine if $p16^{INK4a}$ played a role in wound closure rate, C57/B6 mice at varying ages (5 months and 10 months) with and without *p16,* were wounded and closure was measured. Older mice (10 months old), have an initially slower wound closure than the younger mice (5 months old), regardless of $p16^{INK4a}$ status, suggesting $p16^{INKa}$-independent age-related factors, including other age-dependent cell cycle inhibitors (e.i. ARF) play a role in wound regeneration (Figure 1C).

3.3.2 UV Burn Model

Not only does UV burn healing have a similar pathological phenotype as cutaneous wound healing, UV burns have also been associated with $p16^{INK4a}$ induction. For example, UV light has been shown to cause induction of $p16^{INK4a}$ in cells (Cadet et al., 2005). Additionally, prior work has shown that UV light causes mutagenesis in the Rb pathway, including $p16^{INK4a}$, leading to melanoma (Kannan et al., 2003). To understand how UV exposure affects transient $p16^{INK4a}$ induction, SKH1-E mice were exposed to either 1000 J/m^2 or 2000 J/m^2 then serially imaged for 30 days (Figure 2A). Whole body examination demonstrated redness and edema at site of UV exposure validating an effective dose (Figure 2B). Through imaging analysis, UV light led to dorsal specific induction of $p16^{INK4a}$ starting 2 days after exposure with maximal expression at 4 days with levels 1.75 times higher than baseline (Figure 2, C and D). $p16^{LUC}$ signal is seen at the site of UV exposure, indicating

anatomic specific expression (Figure 2D). These results suggest that UV light leads to a rapid, transient expression of *p16*^{INK4a}.

3.3.3 Pharmacological Modulation of *p16*^{INK4a} transient expression

Pharmacological inhibitors were employed to determine the mechanism of *p16*^{INK4a} transient induction after UV exposure. Others have shown that inflammation can lead to the induction of *p16*^{INK4a} (Freund et al., 2010). Moreover, glucocorticoids, are shown to suppress components of the senescence associated secretory phenotype, including IL-6, IL-8, GM-CSF, and MCP-2 expression (Laberge et al., 2012). *In vivo,* glucocorticoid receptors have been correlated with p16^{INK4a} levels in tumors, suggesting a potential relationship with dexamethasone, a glucocorticoid, and *p16*^{INK4a} expression (Theocharis et al., 2003). However, how dexamethasone affects *p16*^{INK4a} expression after cellular insult is unknown. To address this question, SKH1-E mice were given a daily I.P. injection of dexamethasone every day, starting from the day of UV burn. The mice were then serially imaged for 30 days (Figure 3A). Luciferase signal was recorded and dexamethasone-treated and non-treated mice were compared. Interestingly, dexamethasone treatment hindered induction of *p16*^{INK4a} to almost baseline levels, suggesting an inflammatory response after UV exposure leading to the transient induction of *p16*^{INK4a} (Figure 3B).

Next, we examined the NfκB pathway to further understand the relationship between *p16*^{INK4a} and the inflammatory response during UV burn healing. Prior work has shown that the NfκB pathway plays an important role in the inflammatory response system (Pahl, 1999). Additionally, research has shown that NfkB has a direct relationship with a senescent phenotype in both mice and cells (Rovillain et al., 2011; Tilstra et al., 2012). Moreover,

NfκB in conjunction with p38, a known upstream inducer of $p16^{INK4a}$, regulate the senescence associated secretory phenotype (Freund et al., 2011). To understand the relationship between NfκB and $p16^{INK4a}$ pathways, we treated UV exposed mice with compound A, an IKK-β inhibitor. IKK-β is part of the IKK complex, which is the initial step in the NfκB cascade. By inhibiting IKK complex's ability to phosphorylate the IkB complex, the NfκB pathway is hindered. Our results show mice treated with compound A, every other day starting six days before UV exposure (Figure 3C) exhibited lower $p16^{INK4a}$ induction after UV burn, further strengthening the hypothesis that inflammatory response after UV exposure leads to the induction of $p16^{INK4a}$ (Figure 3D).

Macrophage recruitment during an inflammatory response occurs four days after insult at the peak of $p16^{INK4a}$ induction after UV burn (Figure 2D, (DiPietro, 1995)). Others have shown the $p16^{INK4a}$ is responsible for the activation of tissue macrophage phenotypes (Cudejko et al., 2011; Fuentes et al., 2011), suggesting a role for $p16^{INK4a}$ during macrophage recruitment. Additionally, Cdkn2A, the locus that encodes $p16^{INK4a}$, has been shown to regulate macrophage proliferation (Kuo et al., 2011). To determine if $p16^{INK4a}$ is induced in macrophages during recruitment to the wound, mice were treated with daily I.P. injections of clodrosome, a macrophage depletion compound, starting three days before UV exposure (Figure 4A). Mice were UV burned on day 0, then serially imaged for 30 days. To confirm sufficient depletion, peripheral blood, spleen, and bone marrow were harvested from a cohort of mice on day 4. These cells were stained for specific blood markers, and macrophages were measured using flow cytometry (Figure 4B). Cells that were stained Mac1+F4/80+, known macrophage markers, were then compared between the clodrosome treated and non-treated cohorts. As expected, there was a significant decrease in splenic macrophages, a

modest decrease in peripheral blood macrophages, with no change in bone marrow derived macrophages, validating the data generated from this experiment (Figure 4C). Our imaging results demonstrate the treatment with clodrosome lessened the $p16^{INK4a}$ inducing effects of UV burn, suggesting that macrophages play a role in the transient induction of $p16^{INK4a}$ (Figure 4D).

3.4 Discussion

In this work, we demonstrate through the use of the *p16-LUC* allele, we are able to transiently induce $p16^{INK4a}$ through wounding and UV burns. Moreover, we have effectively modulated expression of $p16^{INK4a}$ after exposure of UV burns by altering the inflammatory response through treatments with dexamethasone, a glucocorticoid, compound A, an IKK-β inhibitor of the NFκB pathway, and clodrosome, a macrophage inhibitor. These data suggest the transient induction of $p16^{INK4a}$ is due to the inflammatory response, potentially through recruitment of macrophages to wound site after a cellular insult, such as a UV burn (Figure 5).

To better understand the relationship between $p16^{INK4a}$ and macrophage infiltration, we plan on completing a series of transplant experiments. Currently, we have clearly demonstrated that $p16^{INK4a}$ is predominantly expressed at the site of insult; however, the cell type is unknown. To confirm the cell type, we plan on transplanting the bone marrow of

mice that have wildtype *p16*^{INK4a} with bone marrow from mice that have heterozygous for the *p16*^{LUC} allele. If there is induction at the site of the insult (luciferase glow at the burn site), *p16*^{INK4a} expression is from the circulating white blood cells. If induction is seen, the white blood cells with be sorted into specific populations using the protocol described, and adoptively transferred into wildtype *p16*^{INK4a} mice, to determine cell specific induction. To strengthen the theory that macrophage infiltration leads to a stronger *p16*^{INK4a} expression, we will inject mice with KRAS transformed cells that have extras copies of colony stimulating factor 1 (CSF-1), a macrophage recruitment signal, and measure tumor growth and luciferase signal. If our hypothesis is correct, then we should see higher levels or faster induction of *p16*^{INK4a} in mice that have the extra CSF-1 when compared to the empty vector controls.

In summary, we have shown that both wounding and UV burn lead to a transient induction of *p16*^{INK4a} with maximum expression at day 4. We have also shown using the UV burn model that inflammatory responses, including macrophage infiltration and induction of the NFκB pathways, affect *p16*^{INK4a} transient expression. While there are many questions that remain unanswered, these experiments develop a platform to better understand *p16*^{INK4a} transient expression *in vivo*.

3.5 Figures

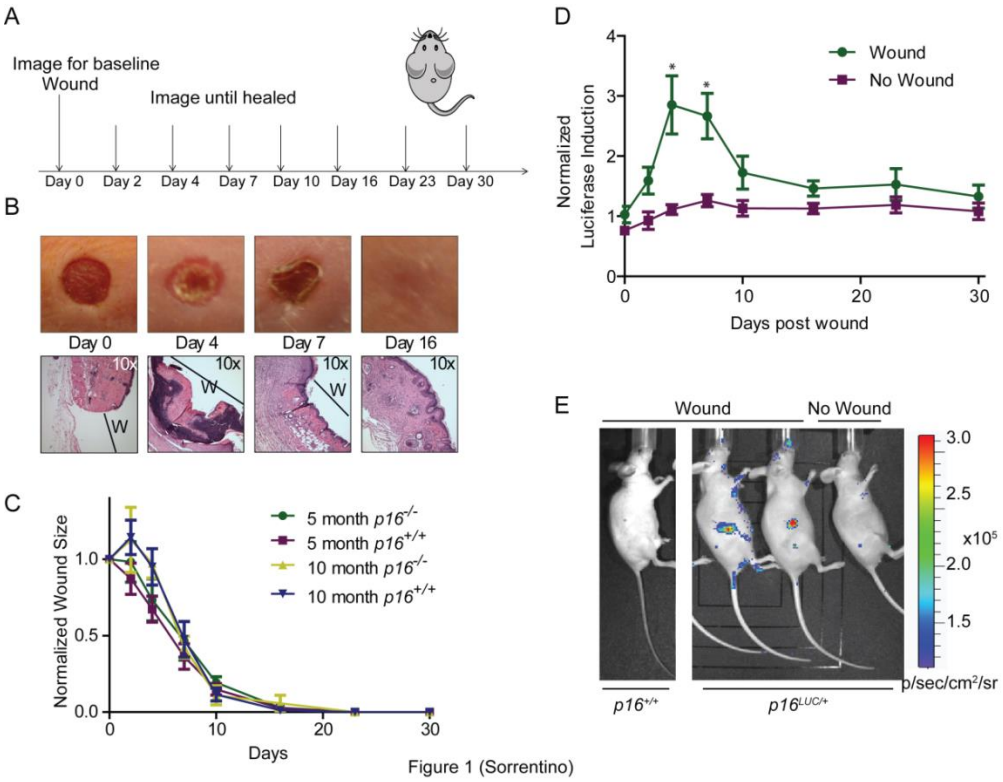

Figure 3.1: Wound healing leads to an induction of *p16^{INK4a}* expression in mice

(A) Model describing the imaging protocol for wounded mice. (B) Gross and histological (stained with hematoxylin and eosin) images of a wound healing up to day 16. (C) Size of wounds in p16-/- and p16+/+ mice graphed as a function of time. Error bars indicate standard error of the mean. (D) Luciferase levels were measured periodically of *p16^{LUC}* wounded mice as measured by TBLI (wound, n=13, no wound, n=9). Luciferase levels were normalized to the mean luciferase levels of the entire cohort at day 0 and graphed as a function of time. (E) Representative images (day 4) of the study described in 'D' are shown. Error bars indicate standard error of the mean. P values were determined through student's t-test analysis. *p<0.05

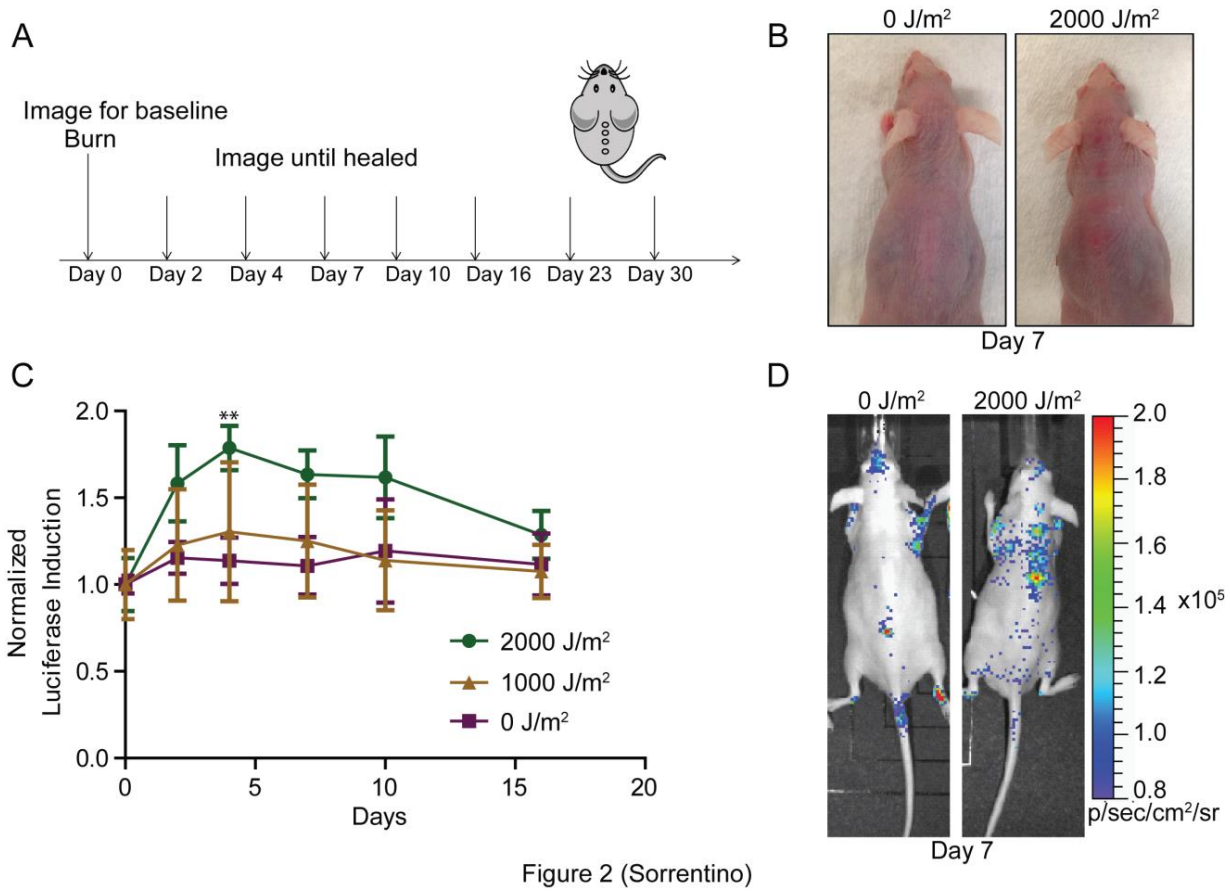

Figure 3.2: UV burn leads to an induction of *p16*^{INK4a} expression in mice

(A) Model describing the imaging protocol for burned mice. (B) Gross images of exposed and non-exposed mice at day 7. (C) Luciferase levels were measured periodically of *p16*^{LUC} mice wound as measured by TBLI (0J/m^2, n=4, 1000 J/m^2, n=5, 2000J/m^2, n=9). Results were recorded, analyzed, and displayed as in Figure 1D. (D) Representative images (day 7) of the study described in 'C" are shown. Error bars indicate standard error of the mean. P values were determined through student's t-test analysis comparing 2000J/m^2 vs. 0J/m^2. **p<0.01

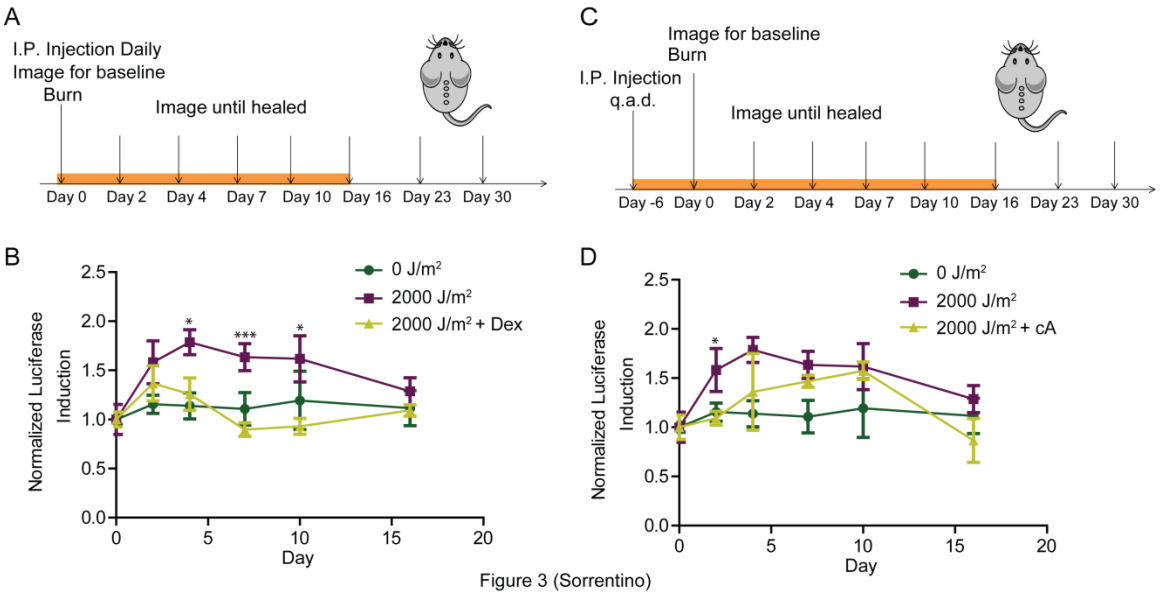

Figure 3.3: Glucocorticosteriod and NfκB inhibitor interfere with the transient induction of *p16^{INK4a}* expression in mice after UV burn

(A) Model describing the imaging and dosing protocol for dexamethasone-treated, burned mice. (B) Luciferase levels were measured periodically of *p16^{LUC}* mice wound as measured by TBLI (0J/m^2, n=4, 2000J/m^2, n=9, Dexamethasone+2000J/m^2, n=4). Results were recorded, analyzed, and displayed as described in Figure 1D. (C) Model describing the imaging and dosing protocol for the IKK-β inhibitor compound A-treated, burned mice. (D) Luciferase levels were measured periodically of *p16^{LUC}* mice wound as measured by TBLI (0J/m^2, n=4, 2000J/m^2, n=9, compoundA+2000J/m^2, n=3). Results were recorded, analyzed, and displayed as described in Figure 1D. Error bars indicate standard error of the mean. P values were determined through student's t-test analysis comparing 2000J/m^2 vs. tmt+2000J/m^2. *p<0.05, ***p<0.001

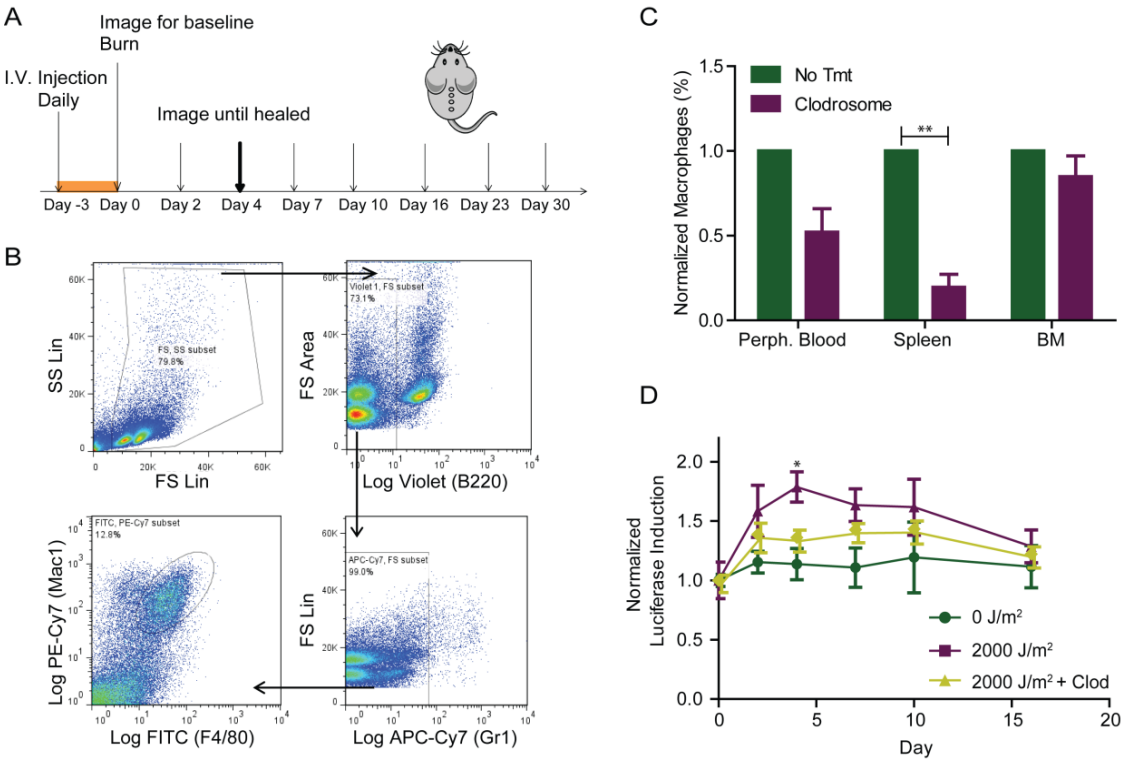

Figure 4 (Sorrentino)

Figure 3.4: Macrophage depletion interferes with the transient induction of *p16^{INK4a}* expression in mice after UV burn

(A) Model describing the imaging and dosing protocol for clodrosome (liposomal clodronate) treated, burned mice. (B) Flow cytometry strategy to determine the macrophage population (Mac1+F4/80+). See methods for further description. (C) Graph depicting the levels of Mac1+F4/80+ cells of clodrosome-treated vs. non-treated in the peripheral blood, spleen, bone marrow (BM) on day 4 (bolded arrow in Figure 4A). (D) Luciferase levels were measured periodically of *p16^{LUC}* mice wound as measured by TBLI (0 J/m^2, n=4, 2000 J/m^2, n=9, clodrosome+2000 J/m^2, n=3). Results were recorded, analyzed, and displayed as described in Figure 1D. Error bars indicate standard error of the mean. P values were determined through student's t-test analysis comparing 2000J/m^2 vs. tmt+2000J/m^2. *p<0.05, **p<0.01

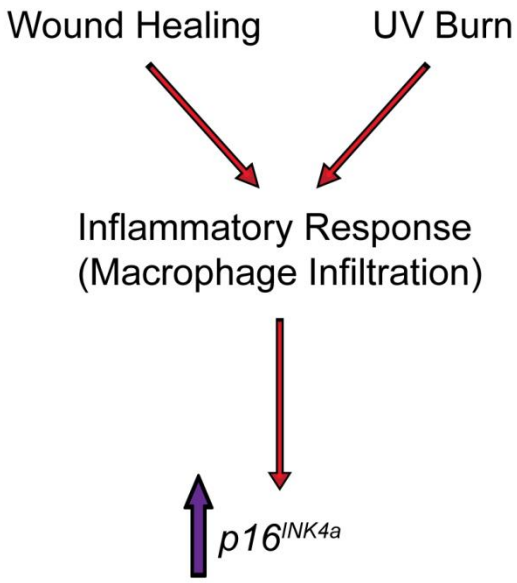

Figure 5 (Sorrentino)

Figure 3.5: A working model of *p16*^{INK4a} induction after wound generation or UV burn.

The wound healing process (after puncture or burn) causes an inflammatory response with a macrophage infiltration by day 4. The inflammation, including the infiltration of macrophages at wound site leads to an induction of *p16*^{INK4a} expression.

CHAPTER 4: OVERALL CONCLUSIONS AND SIGNIFICANCE

4.1 Principal Conclusions

There have been great strides in developing better assays to understand the molecular underpinnings of carcinogens, but the field of gerontogens is not as established. My work describes a way to evaluate the severity of a gerontogen in vivo using a novel mouse model which has allowed us to systemically evaluate four different exposures in mice (Chapter 2). Contrary to the known literature, my work also shows how $p16^{INK4a}$ does not always accumulate in an organism, and might have a niche of transient induction after a wounding event, such as a UV burn (Chapter 3). In summary, my work provides an innovative method for measuring molecular age after chronic exposure to gerontogens and begins to clarify a novel role for $p16^{INK4a}$ transient expression in vivo.

4.2 $p16^{INK4a}$ -Luciferase Allele

Our lab has generated a luciferase reporter allele ($p16^{LUC}$) that measures $p16^{INK4a}$ expression in cancer and aging. Our lab demonstrated that $p16^{INK4a}$ is induced in the stromal

region of a tumor before tumor palpation *in vivo* using the $p16^{LUC}$ allele (Burd et al., 2013). Additionally, we show that the $p16^{LUC}$ allele will detect tumorigenesis in many different tumor types including breast and melanoma. Chapter 2 defines multiple gerontogens and verifies the allele's ability to measure $p16^{INK4a}$-associated aging *in vivo.* In this paper, we also validate the expression of $p16^{INK4a}$ after chronic exposure, and correlated the expression with a senescent phenotype through SA-β gal staining and mRNA expression of SA factors including *Il-6* and *CXCL1*. Currently, we are completing experiments to understand the mechanisms of transient induction of $p16^{INK4a}$ using the $p16^{LUC}$ wound healing model through pharmacological modulation of the $p16^{INK4a}$ expression after a UV burn. The $p16^{LUC}$ reporter allele has made it easier to understand the relationship between $p16^{INK4a}$-associated cancer and aging.

Not only has the $p16^{LUC}$ allele made advancements from a scientific standpoint, this allele is a novel *in vivo* model that can serially measure a specific protein in the same organ over time. Historically, aging *in vivo* studies are very long and expensive since there are tremendous costs for mice, as well as cage costs for having the mice aging for months and possibly years. Additionally, there are incredible costs for the time invested, and proper storage of all tissues after the conclusion of the experiment. By using a mouse model that can measure the protein of interest ($p16^{INK4a}$) in real time, it decreases the costs exponentially and lessens the time commitment significantly.

While the $p16^{LUC}$ allele, as with other luminescent reporter alleles, has furthered scientific knowledge, there are few minor, but important weaknesses that should be addressed. Firstly, there is some individual variation. An individual mouse imaged over a

period of time will show a slow, but steady, induction of luciferase signal correlative with endogenous *p16*^{INK4a} expression. However, this signal will not be linear, with slight spikes and drops throughout the life of the mouse. Additionally, measuring a set of mice at the same time point (e.g. same age) will also yield some variability, which is characteristic of *p16*^{INK4a} expression in human PBTLs (Liu et al., 2009). To fix these issues, internal controls were used per mouse to correct for any background induction (transient exposures), and higher cohort numbers (15+) were used if variability was expected to be higher than normal (e.g. chronic exposures). Secondly, since the luciferase allele required an I.P. injection of luciferin before each image set, technical variation of injection placement, amount of luciferin injected, and time to image taken can also confound results. To address these variations, multiple sets of mice were taken over many months to make sure it was not a dose dependent response of the luciferin. Each image taken included mice from various cohorts if space permitted. To stabilize the time to image variation, experiments were completed to determine steady state of luminescence after injection, which was 8 minutes. Additionally, we determined that 48 hours were needed before mice could be re-imaged with maximal luminescence potential. Mice were also weighed before each luciferin injection to confirm the proper luciferin serum concentrations. Though both minor, these shortcomings were taken into consideration during the course of the studies and addressed to maintain accurate, reliable data.

One major limitation of the *p16*^{LUC} allele is the lack of cellular specifically, making it difficult to detect *p16*^{INK4a} induction in deeper organs or in rare cellular subtypes. For example, the reason for no *p16*^{INK4a} expression differences in the HFD vs. ND (Chapter 2) might be due to the significant age-related changes are in a small subset of cells, such as the

pancreatic β cells, or in a deep organ, such as the aorta or pancreas, making imaging detection difficult. While some validation of luciferase signal correlating with *p16*^{INK4a} mRNA expression was completed in these studies, to completely address this problem, another allele will need to be generated. A new allele will need to encompass the faithful induction of *p16*^{INK4a}, while allowing a level of detection in a single cell. Currently, our lab is generating a second allele that will have a red florescence protein (tdTomato) in place of *p16*^{INK4a} exon 1α, leaving exons 2 and 3 intact, identical to the *p16*^{LUC} allele (Figure 4.1). tdTomato florescence protein was chosen due to its strong signal and limited similarity to auto-florescence during flow cytometry analysis. Ideally, these mice will have the potential to be imaged in real time as well as run flow cytometry analysis on cellular subtypes in order to address those cellular *p16*^{INK4a}-related questions. The *p16*^{INK4a}*-tdTomato* (*p16*^{TOM}) allele will also help us determine whether *p16*^{INK4a} induction is stochastic or gradual among a cellular population. Currently, we don't know if a 50% increase in *p16*^{INK4a} expression means 50% of the cells are expressing 100% of *p16*^{INK4a} expression or if all cells are expressing 50% of the *p16*^{INK4a} expression, and this allele can elucidate those differences. Even though it is thought that *p16*^{INK4a} is only regulated at the transcriptional level, there still might be unanswered questions at the translational level. Both of these alleles will show effects on *p16*^{INK4a} expression at the transcriptional level, leaving the protein regulation in question.

4.3 Theory of gerontogens

George Martin developed a new philosophy about exposures that lead to an aging phenotype and coined the term gerontogens (Martin, 1987). Gerontogens are defined as an exposure that leads to an advanced aging phenotype. While this opened the door to a new thought process about aging toxicology, there were a few questions that were left unanswered; What is an "aging phenotype"? How do you measure aging? Can a gerontogen also be a carcinogen?

An "aging phenotype" implies an array of different theories. Some have described molecular aging as the "lack of proliferative potential" (Kim and Sharpless, 2006), while others considered aging as a diminished lifespan, and often a frailty phenotype (Bryson and Siddiqui, 1969; McMillan and Hubbard, 2012). Aging phenotypes can also include clinical outcomes of the elderly including neuro-degeneration, atherosclerosis, cancer, diabetes, immune suppression, glaucoma, endometriosis, and coronary artery disease (CAD) (Jeck et al., 2012). Interestingly, the molecular mechanisms that lead to these age-related pathologies are vastly different and at times completely opposite. For example, cancer and atherosclerosis are considered highly proliferating disease, while diabetes and neuro-degeneration pathologies are due to lack of regenerating populations of specific cells. To be able to call a toxicant a gerontogen, the aging phenotype must be defined. For the purposes of my studies, I defined gerontogens as toxicants that lead to a lack of cellular regeneration as well as have associations with age-related diseases. For my study, I chose high fat diet (increased susceptibility to diabetes), arsenic (increase susceptibility to diabetes), ultraviolet

light (photo aging, e.g. slower wound repair, lack of elasticity), and cigarette smoke (a wide-array of pathologies, including immune suppression and CAD) as my gerontogen panel.

After gerontogens are defined, there are many ways to measure the aging phenotype, which includes whole organism measurements such as decrease in lifespan and onset of age-related pathologies as described above. As described in the Chapter 1, there are also many different molecular markers to measure the aging phenotype. To utilize our novel $p16^{LUC}$ system, I measured $p16^{INK4a}$ mRNA expression levels as my molecular marker after exposure to the gerontogens of choice. I also tested of validity of $p16^{INK4a}$ expression as an aging marker, and senescence activator, by evaluating *CXCL1* and *IL-6* mRNA levels (SASP factors) as well as SA β-gal stain (senescence marker). The evaluation of $p16^{INK4a}$ expression was successful in measuring aging in certain gerontogens, including UV light and cigarette smoke, but was less successful in measuring the aging phenotype in others, such as arsenic and high fat diet (Chapter 2). While $p16^{INK4a}$ expression showed a modest, but significant change in arsenic exposed mice, the lack of pancreatic islets suggests that arsenic is a stronger gerontogen than we describe. Likewise, even though there were no differences between the mice fed high fat and normal fat diets, it doesn't mean high fat diets can't be considered a gerontogen. As discussed earlier, this can be due to changes in $p16^{INK4a}$ expression in a small subset of cells or deeper organs not detectable by the luciferase system. Additionally, our system is not set up to detect age-related changes other that lack of regeneration, or more specifically changes in $p16^{INK4a}$ expression. Both arsenic and high fat diet might have age-related phenotypes not associated with $p16^{INK4a}$ expression. In fact, both arsenic and high fat have been associated with highly proliferative pathologies,

including atherosclerosis and cancer (Giovannucci and Goldin, 1997; Keys, 1952; Mosby et al., 2012; Nishina et al., 1990; Smith et al., 1992).

Future experiments for this project would take two different directions. Firstly, I would better characterize the "gerontogeness" of the two more dynamic *p16*^{INK4a} expressing gerontogens. I would solidify that exposure to either UV light or cigarette smoke would lead to induction of *p16*^{INK4a}, which leads to a lack of proliferation. For this, cell culture analysis would be employed on organs with the highest levels of *p16*^{INK4a}, including 3T9 cellular passaging assays. Secondly, I would also better define the type of "gerontogeness" the other two less *p16*^{INK4a} associated gerontogens. For this, I would test other markers of aging, including telomere length and oncogene activation. I would also more closely analyze potential specific organs that are hotspots for age-related pathologies. For example, in HFD fed mice, I would look at *p16*^{INK4a} expression in the aorta and pancreatic β cells. In the arsenic exposed mice, I would analyze the pancreatic β cells for *p16*^{INK4a} expression as well as measure characteristics of skin aging including elasticity and wound healing. In summary, detecting changes in *p16*^{INK4a} expression is not the only way to measure aging *in vivo.*

Finally, there is some overlap between "carcinogens" and "gerontogens", including the relationship between both classes and *p16*^{INK4a} expression. As addressed briefly in Chapter 1, cancer is considered an age-related pathology along with other highly proliferative diseases, including atherosclerosis. They occur more frequently at the later stages of life, but the opposite of the "aging" mechanism, or lack of regenerative potential. *p16*^{INK4a} has been shown to be involved with many cancers including melanomas and breast cancer (Herman et al., 1995), while also known to lead to replicative decline in many tissues, such as pancreatic

β cells and neural progenitors (Krishnamurthy et al., 2006; Molofsky et al., 2006). Mechanistically, *p16*^{INK4a} has been shown to be induced after oncogenic stimuli, leading to cell cycle arrest and ultimately senescence, giving this protein tumor suppressor status (Bartkova et al., 2006; Serrano et al., 1997). However, many tumors have *p16*^{INK4a} silenced, through methylation of the promoter for example, allowing the cell to bypass the tumor suppression and hyper proliferate leading to cancer (Herman et al., 1995). DNA damage, either direct or indirect, has also been shown to induce *p16*^{INK4a} as described in Chapter 2. Chronic DNA damage can also lead to suppression of the *CDN2A* locus, allowing the transition into a tumorigenic state (e.g. UV light-induced melanoma) (Kannan et al., 2003). The commonality with the different relationships of *p16*^{INK4a} induction and cancer is that somehow the original insult, whether it is oncogenic stimuli or DNA damaging agent, causes an induction of *p16*^{INK4a} to senesce the cell before transition into a malignant state. The mechanism as to how the cells moves from extremely high levels of *p16*^{INK4a} to a silenced *CDKN2A* locus, bypassed senescent state, and subsequently tumorigenesis is still unclear. Additionally, our group has shown the *p16*^{INK4a} is produced in the stromal cells around a tumor, suggesting some signal for normal cells to stop proliferating. As my recent work proposes (Chapter 3), macrophage infiltration with high levels of *p16*^{INK4a} expression may explain the influx of *p16*^{INK4a} localized around the tumor or wound.

4.4 *p16*^{INK4a} regulation in vivo

As described above, p16^{INK4a} is a tumor suppressor that regulates the G1 to S phase transition of the cell cycle through the RB pathway (Kim and Sharpless, 2006). While it is

known that $p16^{INK4a}$ expression leads to a permanent growth arrest, it is still unclear how the cell switches from a paused state in the cell cycle to a senescent state. A tremendous effort has been made to determine the regulation of $p16^{INK4a}$ expression. Prior work has shown that many transcription factors, including the polycomb group proteins, contribute to $p16^{INK4a}$ modulation (Bracken et al., 2007). The immediate upstream transcription factors have been discovered, however, relationship between environmental exposure and modulation of transcription factors remains unclear. Moreover, very little work has been completed to understand the transient induction *in vivo*.

Our newest experiments have shown that $p16^{INK4a}$ is transiently induced four days after a wound is generated (Chapter 3). The transient induction can be caused by one or a combination of the following hypotheses: 1) transcription factors that regulate $p16^{INK4a}$ expression to turn on momentarily, 2) there is an influx of a specific cell type that has high level of $p16^{INK4a}$ to the wound site, suggesting a concentrated induction, and 3) the cells are recruited to the site of insult, then leading to an induction of $p16^{INK4a}$. There is strong evidence to show that $p16^{INK4a}$ accumulates over time in both mice and humans with no translational repression, suggesting that our first hypothesis is possibly but unprecedented (Krishnamurthy et al., 2004; Liu et al., 2009). Both our second and third hypotheses seem plausible especially with our data indicating a relationship between $p16^{INK4a}$ transient expression and an inflammatory response.

As described in Chapter 3, we have recently determined that transient $p16^{INK4a}$ expression after UV wound exposure is ablated through disruption of the inflammatory process. Moreover, macrophage depletion hindered $p16^{INK4a}$ expression by half after wound

generation. Additionally, peak induction of *p16*^{INK4a} induction correlates with macrophage infiltration during wound healing (Leibovich and Ross, 1975), suggesting *p16*^{INK4a} regulation is dependent on macrophage recruitment during an inflammatory response. The experiments described in Chapter 3 will help solidify our hypothesis that *p16*^{INK4a} is found in the macrophages at the site of cellular insult, however, they will not determine if the macrophages have high levels of *p16*^{INK4a} before recruitment to injury or once macrophages reach the wound site then *p16*^{INK4a} expression occurs. Potentially, single cell tracking can be employed to determine the *p16*^{INK4a} expression mechanism during macrophage recruitment. Additionally, further experimentation is necessary to determine if *p16*^{INK4a} is required for proper wound healing or rather simply a biomarker for the inflammatory response.

4.5 Importance and Significance

This work has given the field a new, cost effective method for understanding how *p16*^{INK4a} expression correlates with chronic exposures *in vivo*. These studies also further the relationship between *p16*^{INK4a} expression, senescence and aging (Chapter 2). By better understanding the molecular mechanisms of aging, we can work towards better therapeutics of age-related diseases as well as lessen some of the effects after chronic exposures over a lifetime. My work has also scratched the surface of the mechanism for transient induction of *p16*^{INK4a} expression *in vivo*. The completed UV wound healing work along with my future experiments will demonstrate how *p16*^{INK4a} is transiently induced and will give us a platform to learn why *p16*^{INK4a} induction is necessary during a would repair response. Eventually, this

work can help bridge the connection between *p16*^{INK4a} expression, chronic injury, and *p16*^{INK4a} -associated cancer and aging pathologies.

4.6 Figures

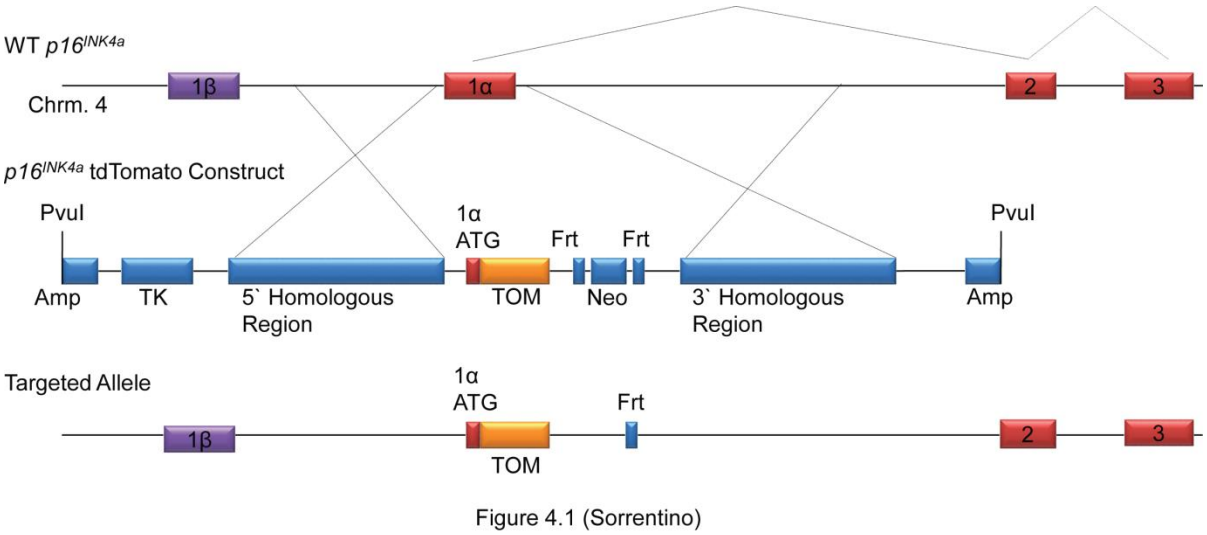

Figure 4.1 (Sorrentino)

Figure 4. 1 Design of of *p16^{TOM}* allele

Schematic of the *p16^{TOM}* knockin targeting strategy. "Targeted allele" denotes the allele after Flp-recombinase-mediated excision of the neomycin selection cassette.

REFERENCES

Andrew, A.S., Burgess, J.L., Meza, M.M., Demidenko, E., Waugh, M.G., Hamilton, J.W., and Karagas, M.R. (2006). Arsenic exposure is associated with decreased DNA repair in vitro and in individuals exposed to drinking water arsenic. Environmental health perspectives *114*, 1193-1198.

Andrew, A.S., Karagas, M.R., and Hamilton, J.W. (2003). Decreased DNA repair gene expression among individuals exposed to arsenic in United States drinking water. International journal of cancer Journal international du cancer *104*, 263-268.

Baker, D.J., Wijshake, T., Tchkonia, T., LeBrasseur, N.K., Childs, B.G., van de Sluis, B., Kirkland, J.L., and van Deursen, J.M. (2011). Clearance of p16Ink4a-positive senescent cells delays ageing-associated disorders. Nature *479*, 232-236.

Banerjee, M., Sarma, N., Biswas, R., Roy, J., Mukherjee, A., and Giri, A.K. (2008). DNA repair deficiency leads to susceptibility to develop arsenic-induced premalignant skin lesions. International journal of cancer Journal international du cancer *123*, 283-287.

Bartkova, J., Rezaei, N., Liontos, M., Karakaidos, P., Kletsas, D., Issaeva, N., Vassiliou, L.V., Kolettas, E., Niforou, K., Zoumpourlis, V.C., *et al.* (2006). Oncogene-induced senescence is part of the tumorigenesis barrier imposed by DNA damage checkpoints. Nature *444*, 633-637.

Belluzzi, J.D., Lee, A.G., Oliff, H.S., and Leslie, F.M. (2004). Age-dependent effects of nicotine on locomotor activity and conditioned place preference in rats. Psychopharmacology *174*, 389-395.

Berent-Maoz, B., Montecino-Rodriguez, E., Signer, R.A., and Dorshkind, K. (2012). Fibroblast growth factor-7 partially reverses murine thymocyte progenitor aging by repression of Ink4a. Blood *119*, 5715-5721.

Bernhard, D., Moser, C., Backovic, A., and Wick, G. (2007). Cigarette smoke--an aging accelerator? Experimental gerontology *42*, 160-165.

Bracken, A.P., Kleine-Kohlbrecher, D., Dietrich, N., Pasini, D., Gargiulo, G., Beekman, C., Theilgaard-Monch, K., Minucci, S., Porse, B.T., Marine, J.C., *et al.* (2007). The Polycomb group proteins bind throughout the INK4A-ARF locus and are disassociated in senescent cells. Genes & development *21*, 525-530.

Bradshaw, A.D., Reed, M.J., and Sage, E.H. (2002). SPARC-null mice exhibit accelerated cutaneous wound closure. The journal of histochemistry and cytochemistry : official journal of the Histochemistry Society *50*, 1-10.

Bruunsgaard, H., Pedersen, M., and Pedersen, B.K. (2001). Aging and proinflammatory cytokines. Current opinion in hematology *8*, 131-136.

Bryson, M.C., and Siddiqui, M.M. (1969). Some Criteria for Aging. J Am Stat Assoc *64*, 1472-&.

Burd, C.E., Jeck, W.R., Liu, Y., Sanoff, H.K., Wang, Z., and Sharpless, N.E. (2010). Expression of linear and novel circular forms of an INK4/ARF-associated non-coding RNA correlates with atherosclerosis risk. PLoS genetics *6*, e1001233.

Burd, C.E., Sorrentino, J.A., Clark, K.S., Darr, D.B., Krishnamurthy, J., Deal, A.M., Bardeesy, N., Castrillon, D.H., Beach, D.H., and Sharpless, N.E. (2013). Monitoring tumorigenesis and senescence in vivo with a p16(INK4a)-luciferase model. Cell *152*, 340-351.

Cadet, J., Sage, E., and Douki, T. (2005). Ultraviolet radiation-mediated damage to cellular DNA. Mutation research *571*, 3-17.

Campisi, J., and d'Adda di Fagagna, F. (2007). Cellular senescence: when bad things happen to good cells. Nature reviews Molecular cell biology *8*, 729-740.

Cesari, M., Penninx, B.W., Pahor, M., Lauretani, F., Corsi, A.M., Rhys Williams, G., Guralnik, J.M., and Ferrucci, L. (2004). Inflammatory markers and physical performance in older persons: the InCHIANTI study. The journals of gerontology Series A, Biological sciences and medical sciences *59*, 242-248.

Chavous, D.A., Jackson, F.R., and O'Connor, C.M. (2001). Extension of the Drosophila lifespan by overexpression of a protein repair methyltransferase. Proceedings of the National Academy of Sciences of the United States of America *98*, 14814-14818.

Chen, H., Gu, X., Liu, Y., Wang, J., Wirt, S.E., Bottino, R., Schorle, H., Sage, J., and Kim, S.K. (2011a). PDGF signalling controls age-dependent proliferation in pancreatic beta-cells. Nature *478*, 349-355.

Chen, H., Gu, X., Su, I.H., Bottino, R., Contreras, J.L., Tarakhovsky, A., and Kim, S.K. (2009). Polycomb protein Ezh2 regulates pancreatic beta-cell Ink4a/Arf expression and regeneration in diabetes mellitus. Genes & development *23*, 975-985.

Chen, J.H., Stoeber, K., Kingsbury, S., Ozanne, S.E., Williams, G.H., and Hales, C.N. (2004). Loss of proliferative capacity and induction of senescence in oxidatively stressed human fibroblasts. The Journal of biological chemistry *279*, 49439-49446.

Chen, W., Kimura, M., Kim, S., Cao, X., Srinivasan, S.R., Berenson, G.S., Kark, J.D., and Aviv, A. (2011b). Longitudinal versus cross-sectional evaluations of leukocyte telomere length dynamics: age-dependent telomere shortening is the rule. The journals of gerontology Series A, Biological sciences and medical sciences *66*, 312-319.

Cohen, H.J., Pieper, C.F., Harris, T., Rao, K.M., and Currie, M.S. (1997). The association of plasma IL-6 levels with functional disability in community-dwelling elderly. The journals of gerontology Series A, Biological sciences and medical sciences *52*, M201-208.

Coppe, J.P., Desprez, P.Y., Krtolica, A., and Campisi, J. (2010). The senescence-associated secretory phenotype: the dark side of tumor suppression. Annual review of pathology *5*, 99-118.

Cudejko, C., Wouters, K., Fuentes, L., Hannou, S.A., Paquet, C., Bantubungi, K., Bouchaert, E., Vanhoutte, J., Fleury, S., Remy, P., *et al.* (2011). p16INK4a deficiency promotes IL-4-

induced polarization and inhibits proinflammatory signaling in macrophages. Blood *118*, 2556-2566.

d'Adda di Fagagna, F., Reaper, P.M., Clay-Farrace, L., Fiegler, H., Carr, P., Von Zglinicki, T., Saretzki, G., Carter, N.P., and Jackson, S.P. (2003). A DNA damage checkpoint response in telomere-initiated senescence. Nature *426*, 194-198.

Dai, C.Y., and Enders, G.H. (2000). p16 INK4a can initiate an autonomous senescence program. Oncogene *19*, 1613-1622.

Davalos, A.R., Coppe, J.P., Campisi, J., and Desprez, P.Y. (2010). Senescent cells as a source of inflammatory factors for tumor progression. Cancer metastasis reviews *29*, 273-283.

Deelen, J., Uh, H.W., Monajemi, R., van Heemst, D., Thijssen, P.E., Bohringer, S., van den Akker, E.B., de Craen, A.J., Rivadeneira, F., Uitterlinden, A.G., *et al.* (2013). Gene set analysis of GWAS data for human longevity highlights the relevance of the insulin/IGF-1 signaling and telomere maintenance pathways. Age (Dordr) *35*, 235-249.

DeMarini, D.M. (2004). Genotoxicity of tobacco smoke and tobacco smoke condensate: a review. Mutation research *567*, 447-474.

Dimri, G.P., Lee, X., Basile, G., Acosta, M., Scott, G., Roskelley, C., Medrano, E.E., Linskens, M., Rubelj, I., Pereira-Smith, O., *et al.* (1995). A biomarker that identifies senescent human cells in culture and in aging skin in vivo. Proceedings of the National Academy of Sciences of the United States of America *92*, 9363-9367.

DiPietro, L.A. (1995). Wound healing: the role of the macrophage and other immune cells. Shock *4*, 233-240.

Dix, D.J., Houck, K.A., Martin, M.T., Richard, A.M., Setzer, R.W., and Kavlock, R.J. (2007). The ToxCast program for prioritizing toxicity testing of environmental chemicals. Toxicological sciences : an official journal of the Society of Toxicology *95*, 5-12.

Ershler, W.B., and Keller, E.T. (2000). Age-associated increased interleukin-6 gene expression, late-life diseases, and frailty. Annual review of medicine *51*, 245-270.

Fisher, G.J., Kang, S., Varani, J., Bata-Csorgo, Z., Wan, Y., Datta, S., and Voorhees, J.J. (2002). Mechanisms of photoaging and chronological skin aging. Archives of dermatology *138*, 1462-1470.

Fleming, A., Sato, M., and Goldsmith, P. (2005). High-throughput in vivo screening for bone anabolic compounds with zebrafish. Journal of biomolecular screening *10*, 823-831.

Frankel, S., Ziafazeli, T., and Rogina, B. (2011). dSir2 and longevity in Drosophila. Experimental gerontology *46*, 391-396.

Freund, A., Orjalo, A.V., Desprez, P.Y., and Campisi, J. (2010). Inflammatory networks during cellular senescence: causes and consequences. Trends in molecular medicine *16*, 238-246.

Freund, A., Patil, C.K., and Campisi, J. (2011). p38MAPK is a novel DNA damage response-independent regulator of the senescence-associated secretory phenotype. The EMBO journal *30*, 1536-1548.

Frost, S.J., Simpson, D.J., Clayton, R.N., and Farrell, W.E. (1999). Transfection of an inducible p16/CDKN2A construct mediates reversible growth inhibition and G1 arrest in the AtT20 pituitary tumor cell line. Mol Endocrinol *13*, 1801-1810.

Fuentes, L., Wouters, K., Hannou, S.A., Cudejko, C., Rigamonti, E., Mayi, T.H., Derudas, B., Pattou, F., Chinetti-Gbaguidi, G., Staels, B., *et al.* (2011). Downregulation of the tumour suppressor p16INK4A contributes to the polarisation of human macrophages toward an adipose tissue macrophage (ATM)-like phenotype. Diabetologia *54*, 3150-3156.

Gerhard, G.S., and Cheng, K.C. (2002). A call to fins! Zebrafish as a gerontological model. Aging cell *1*, 104-111.

Gilchrest, B.A., Stoff, J.S., and Soter, N.A. (1982). Chronologic aging alters the response to ultraviolet-induced inflammation in human skin. The Journal of investigative dermatology *79*, 11-15.

Giovannucci, E., and Goldin, B. (1997). The role of fat, fatty acids, and total energy intake in the etiology of human colon cancer. The American journal of clinical nutrition *66*, 1564S-1571S.

Goldsworthy, T.L., Recio, L., Brown, K., Donehower, L.A., Mirsalis, J.C., Tennant, R.W., and Purchase, I.F. (1994). Transgenic animals in toxicology. Fundamental and applied toxicology : official journal of the Society of Toxicology *22*, 8-19.

Gosain, A., and DiPietro, L.A. (2004). Aging and wound healing. World journal of surgery *28*, 321-326.

Grivennikov, S., Karin, E., Terzic, J., Mucida, D., Yu, G.Y., Vallabhapurapu, S., Scheller, J., Rose-John, S., Cheroutre, H., Eckmann, L., *et al.* (2009). IL-6 and Stat3 are required for survival of intestinal epithelial cells and development of colitis-associated cancer. Cancer cell *15*, 103-113.

Gruber, J., Ng, L.F., Poovathingal, S.K., and Halliwell, B. (2009). Deceptively simple but simply deceptive--Caenorhabditis elegans lifespan studies: considerations for aging and antioxidant effects. FEBS letters *583*, 3377-3387.

Hager, K., Machein, U., Krieger, S., Platt, D., Seefried, G., and Bauer, J. (1994). Interleukin-6 and selected plasma proteins in healthy persons of different ages. Neurobiology of aging *15*, 771-772.

Harrison, D.E., Strong, R., Sharp, Z.D., Nelson, J.F., Astle, C.M., Flurkey, K., Nadon, N.L., Wilkinson, J.E., Frenkel, K., Carter, C.S., *et al.* (2009). Rapamycin fed late in life extends lifespan in genetically heterogeneous mice. Nature *460*, 392-395.

Hartwig, A., Groblinghoff, U.D., Beyersmann, D., Natarajan, A.T., Filon, R., and Mullenders, L.H. (1997). Interaction of arsenic(III) with nucleotide excision repair in UV-irradiated human fibroblasts. Carcinogenesis *18*, 399-405.

Hayflick, L., and Moorhead, P.S. (1961). The serial cultivation of human diploid cell strains. Experimental cell research *25*, 585-621.

Herman, J.G., Merlo, A., Mao, L., Lapidus, R.G., Issa, J.P., Davidson, N.E., Sidransky, D., and Baylin, S.B. (1995). Inactivation of the CDKN2/p16/MTS1 gene is frequently associated with aberrant DNA methylation in all common human cancers. Cancer research *55*, 4525-4530.

Hodge, D.R., Hurt, E.M., and Farrar, W.L. (2005). The role of IL-6 and STAT3 in inflammation and cancer. Eur J Cancer *41*, 2502-2512.

Hsu, A.L., Murphy, C.T., and Kenyon, C. (2003). Regulation of aging and age-related disease by DAF-16 and heat-shock factor. Science *300*, 1142-1145.

Impola, U., Jeskanen, L., Ravanti, L., Syrjanen, S., Baldursson, B., Kahari, V.M., and Saarialho-Kere, U. (2005). Expression of matrix metalloproteinase (MMP)-7 and MMP-13 and loss of MMP-19 and p16 are associated with malignant progression in chronic wounds. The British journal of dermatology *152*, 720-726.

Ito, K., and Barnes, P.J. (2009). COPD as a disease of accelerated lung aging. Chest *135*, 173-180.

Jacobs, J.J., Kieboom, K., Marino, S., DePinho, R.A., and van Lohuizen, M. (1999). The oncogene and Polycomb-group gene bmi-1 regulates cell proliferation and senescence through the ink4a locus. Nature *397*, 164-168.

Jacobson-Kram, D., Sistare, F.D., and Jacobs, A.C. (2004). Use of transgenic mice in carcinogenicity hazard assessment. Toxicologic pathology *32 Suppl 1*, 49-52.

Janzen, V., Forkert, R., Fleming, H.E., Saito, Y., Waring, M.T., Dombkowski, D.M., Cheng, T., DePinho, R.A., Sharpless, N.E., and Scadden, D.T. (2006). Stem-cell ageing modified by the cyclin-dependent kinase inhibitor p16INK4a. Nature *443*, 421-426.

Jeck, W.R., Siebold, A.P., and Sharpless, N.E. (2012). Review: a meta-analysis of GWAS and age-associated diseases. Aging cell *11*, 727-731.

Jun, J.I., and Lau, L.F. (2010a). Cellular senescence controls fibrosis in wound healing. Aging *2*, 627-631.

Jun, J.I., and Lau, L.F. (2010b). The matricellular protein CCN1 induces fibroblast senescence and restricts fibrosis in cutaneous wound healing. Nature cell biology *12*, 676-685.

Kannan, K., Sharpless, N.E., Xu, J., O'Hagan, R.C., Bosenberg, M., and Chin, L. (2003). Components of the Rb pathway are critical targets of UV mutagenesis in a murine melanoma model. Proceedings of the National Academy of Sciences of the United States of America *100*, 1221-1225.

Kapaj, S., Peterson, H., Liber, K., and Bhattacharya, P. (2006). Human health effects from chronic arsenic poisoning--a review. Journal of environmental science and health Part A, Toxic/hazardous substances & environmental engineering *41*, 2399-2428.

Keys, A. (1952). Human atherosclerosis and the diet. Circulation *5*, 115-118.

Kharitonov, S.A., Robbins, R.A., Yates, D., Keatings, V., and Barnes, P.J. (1995). Acute and chronic effects of cigarette smoking on exhaled nitric oxide. American journal of respiratory and critical care medicine *152*, 609-612.

Kiel, M.J., Yilmaz, O.H., Iwashita, T., Terhorst, C., and Morrison, S.J. (2005). SLAM family receptors distinguish hematopoietic stem and progenitor cells and reveal endothelial niches for stem cells. Cell *121*, 1109-1121.

Kim, W.Y., and Sharpless, N.E. (2006). The regulation of INK4/ARF in cancer and aging. Cell *127*, 265-275.

Kligman, L.H. (1989). Photoaging. Manifestations, prevention, and treatment. Clinics in geriatric medicine *5*, 235-251.

Kotake, Y., Cao, R., Viatour, P., Sage, J., Zhang, Y., and Xiong, Y. (2007). pRB family proteins are required for H3K27 trimethylation and Polycomb repression complexes binding to and silencing p16INK4alpha tumor suppressor gene. Genes & development *21*, 49-54.

Krishnamurthy, J., Ramsey, M.R., Ligon, K.L., Torrice, C., Koh, A., Bonner-Weir, S., and Sharpless, N.E. (2006). p16INK4a induces an age-dependent decline in islet regenerative potential. Nature *443*, 453-457.

Krishnamurthy, J., Torrice, C., Ramsey, M.R., Kovalev, G.I., Al-Regaiey, K., Su, L., and Sharpless, N.E. (2004). Ink4a/Arf expression is a biomarker of aging. J Clin Invest *114*, 1299-1307.

Krtolica, A., Parrinello, S., Lockett, S., Desprez, P.Y., and Campisi, J. (2001). Senescent fibroblasts promote epithelial cell growth and tumorigenesis: a link between cancer and aging. Proceedings of the National Academy of Sciences of the United States of America *98*, 12072-12077.

Kuilman, T., Michaloglou, C., Vredeveld, L.C., Douma, S., van Doorn, R., Desmet, C.J., Aarden, L.A., Mooi, W.J., and Peeper, D.S. (2008). Oncogene-induced senescence relayed by an interleukin-dependent inflammatory network. Cell *133*, 1019-1031.

Kuo, C.L., Murphy, A.J., Sayers, S., Li, R., Yvan-Charvet, L., Davis, J.Z., Krishnamurthy, J., Liu, Y., Puig, O., Sharpless, N.E., *et al.* (2011). Cdkn2a is an atherosclerosis modifier locus that regulates monocyte/macrophage proliferation. Arteriosclerosis, thrombosis, and vascular biology *31*, 2483-2492.

Laberge, R.M., Zhou, L., Sarantos, M.R., Rodier, F., Freund, A., de Keizer, P.L., Liu, S., Demaria, M., Cong, Y.S., Kapahi, P., *et al.* (2012). Glucocorticoids suppress selected components of the senescence-associated secretory phenotype. Aging cell *11*, 569-578.

Lakin, N.D., and Jackson, S.P. (1999). Regulation of p53 in response to DNA damage. Oncogene *18*, 7644-7655.

Lazar-Molnar, E., Hegyesi, H., Toth, S., and Falus, A. (2000). Autocrine and paracrine regulation by cytokines and growth factors in melanoma. Cytokine *12*, 547-554.

Leibovich, S.J., and Ross, R. (1975). The role of the macrophage in wound repair. A study with hydrocortisone and antimacrophage serum. The American journal of pathology *78*, 71-100.

Liang, H., Masoro, E.J., Nelson, J.F., Strong, R., McMahan, C.A., and Richardson, A. (2003). Genetic mouse models of extended lifespan. Experimental gerontology *38*, 1353-1364.

Lin, J., Epel, E., Cheon, J., Kroenke, C., Sinclair, E., Bigos, M., Wolkowitz, O., Mellon, S., and Blackburn, E. (2010). Analyses and comparisons of telomerase activity and telomere length in human T and B cells: insights for epidemiology of telomere maintenance. Journal of immunological methods *352*, 71-80.

Liu, Y., Johnson, S.M., Fedoriw, Y., Rogers, A.B., Yuan, H., Krishnamurthy, J., and Sharpless, N.E. (2011). Expression of p16(INK4a) prevents cancer and promotes aging in lymphocytes. Blood *117*, 3257-3267.

Liu, Y., Sanoff, H.K., Cho, H., Burd, C.E., Torrice, C., Ibrahim, J.G., Thomas, N.E., and Sharpless, N.E. (2009). Expression of p16(INK4a) in peripheral blood T-cells is a biomarker of human aging. Aging cell *8*, 439-448.

Long, G.G., Morton, D., Peters, T., Short, B., and Skydsgaard, M. (2010). Alternative mouse models for carcinogenicity assessment: industry use and issues with pathology interpretation. Toxicologic pathology *38*, 43-50.

Longo, D.L. (2009). Telomere dynamics in aging: much ado about nothing? The journals of gerontology Series A, Biological sciences and medical sciences *64*, 963-964.

Maggio, M., Guralnik, J.M., Longo, D.L., and Ferrucci, L. (2006). Interleukin-6 in aging and chronic disease: a magnificent pathway. The journals of gerontology Series A, Biological sciences and medical sciences *61*, 575-584.

Martin, G.M. (1987). Interactions of aging and environmental agents: the gerontological perspective. Progress in clinical and biological research *228*, 25-80.

Martin, P. (1997). Wound healing--aiming for perfect skin regeneration. Science *276*, 75-81.

Masoro, E.J. (2000). Caloric restriction and aging: an update. Experimental gerontology *35*, 299-305.

Matheu, A., Maraver, A., and Serrano, M. (2008). The Arf/p53 pathway in cancer and aging. Cancer research *68*, 6031-6034.

Matheu, A., Pantoja, C., Efeyan, A., Criado, L.M., Martin-Caballero, J., Flores, J.M., Klatt, P., and Serrano, M. (2004). Increased gene dosage of Ink4a/Arf results in cancer resistance and normal aging. Genes & development *18*, 2736-2746.

McCarroll, S.A., Murphy, C.T., Zou, S., Pletcher, S.D., Chin, C.S., Jan, Y.N., Kenyon, C., Bargmann, C.I., and Li, H. (2004). Comparing genomic expression patterns across species identifies shared transcriptional profile in aging. Nature genetics *36*, 197-204.

McMillan, G.J., and Hubbard, R.E. (2012). Frailty in older inpatients: what physicians need to know. QJM : monthly journal of the Association of Physicians *105*, 1059-1065.

Melk, A., Schmidt, B.M., Takeuchi, O., Sawitzki, B., Rayner, D.C., and Halloran, P.F. (2004). Expression of p16INK4a and other cell cycle regulator and senescence associated genes in aging human kidney. Kidney international *65*, 510-520.

Meng, A., Wang, Y., Van Zant, G., and Zhou, D. (2003). Ionizing radiation and busulfan induce premature senescence in murine bone marrow hematopoietic cells. Cancer research *63*, 5414-5419.

Migliore, L., and Coppede, F. (2009). Environmental-induced oxidative stress in neurodegenerative disorders and aging. Mutation research *674*, 73-84.

Miller, R.A., Harrison, D.E., Astle, C.M., Floyd, R.A., Flurkey, K., Hensley, K.L., Javors, M.A., Leeuwenburgh, C., Nelson, J.F., Ongini, E., *et al.* (2007). An Aging Interventions Testing Program: study design and interim report. Aging cell *6*, 565-575.

Mirabello, L., Huang, W.Y., Wong, J.Y., Chatterjee, N., Reding, D., Crawford, E.D., De Vivo, I., Hayes, R.B., and Savage, S.A. (2009). The association between leukocyte telomere length and cigarette smoking, dietary and physical variables, and risk of prostate cancer. Aging cell *8*, 405-413.

Mollica, L., Fleury, I., Belisle, C., Provost, S., Roy, D.C., and Busque, L. (2009). No association between telomere length and blood cell counts in elderly individuals. The journals of gerontology Series A, Biological sciences and medical sciences *64*, 965-967.

Molofsky, A.V., Slutsky, S.G., Joseph, N.M., He, S., Pardal, R., Krishnamurthy, J., Sharpless, N.E., and Morrison, S.J. (2006). Increasing p16INK4a expression decreases forebrain progenitors and neurogenesis during ageing. Nature *443*, 448-452.

Mosby, T.T., Cosgrove, M., Sarkardei, S., Platt, K.L., and Kaina, B. (2012). Nutrition in adult and childhood cancer: role of carcinogens and anti-carcinogens. Anticancer research *32*, 4171-4192.

Muezzinler, A., Zaineddin, A.K., and Brenner, H. (2013). A systematic review of leukocyte telomere length and age in adults. Ageing research reviews *12*, 509-519.

Natarajan, E., Omobono, J.D., 2nd, Guo, Z., Hopkinson, S., Lazar, A.J., Brenn, T., Jones, J.C., and Rheinwald, J.G. (2006). A keratinocyte hypermotility/growth-arrest response involving laminin 5 and p16INK4A activated in wound healing and senescence. The American journal of pathology *168*, 1821-1837.

Natarajan, E., Omobono, J.D., 2nd, Jones, J.C., and Rheinwald, J.G. (2005). Co-expression of p16INK4A and laminin 5 by keratinocytes: a wound-healing response coupling hypermotility with growth arrest that goes awry during epithelial neoplastic progression. The journal of investigative dermatology Symposium proceedings / the Society for Investigative Dermatology, Inc [and] European Society for Dermatological Research *10*, 72-85.

Natarajan, E., Saeb, M., Crum, C.P., Woo, S.B., McKee, P.H., and Rheinwald, J.G. (2003). Co-expression of p16(INK4A) and laminin 5 gamma2 by microinvasive and superficial

squamous cell carcinomas in vivo and by migrating wound and senescent keratinocytes in culture. The American journal of pathology *163*, 477-491.

Nelson, J.A., Krishnamurthy, J., Menezes, P., Liu, Y., Hudgens, M.G., Sharpless, N.E., and Eron, J.J., Jr. (2012). Expression of p16(INK4a) as a biomarker of T-cell aging in HIV-infected patients prior to and during antiretroviral therapy. Aging cell *11*, 916-918.

Nielsen, G.P., Stemmer-Rachamimov, A.O., Shaw, J., Roy, J.E., Koh, J., and Louis, D.N. (1999). Immunohistochemical survey of p16INK4A expression in normal human adult and infant tissues. Laboratory investigation; a journal of technical methods and pathology *79*, 1137-1143.

Nishina, P.M., Verstuyft, J., and Paigen, B. (1990). Synthetic low and high fat diets for the study of atherosclerosis in the mouse. Journal of lipid research *31*, 859-869.

Ohtani, N., Zebedee, Z., Huot, T.J., Stinson, J.A., Sugimoto, M., Ohashi, Y., Sharrocks, A.D., Peters, G., and Hara, E. (2001). Opposing effects of Ets and Id proteins on p16INK4a expression during cellular senescence. Nature *409*, 1067-1070.

Pahl, H.L. (1999). Activators and target genes of Rel/NF-kappaB transcription factors. Oncogene *18*, 6853-6866.

Paul, D.S., Harmon, A.W., Devesa, V., Thomas, D.J., and Styblo, M. (2007). Molecular mechanisms of the diabetogenic effects of arsenic: inhibition of insulin signaling by arsenite and methylarsonous acid. Environmental health perspectives *115*, 734-742.

Pavey, S., Conroy, S., Russell, T., and Gabrielli, B. (1999). Ultraviolet radiation induces p16CDKN2A expression in human skin. Cancer research *59*, 4185-4189.

Pfeifer, G.P., Denissenko, M.F., Olivier, M., Tretyakova, N., Hecht, S.S., and Hainaut, P. (2002). Tobacco smoke carcinogens, DNA damage and p53 mutations in smoking-associated cancers. Oncogene *21*, 7435-7451.

Piao, F., Ma, N., Hiraku, Y., Murata, M., Oikawa, S., Cheng, F., Zhong, L., Yamauchi, T., Kawanishi, S., and Yokoyama, K. (2005). Oxidative DNA damage in relation to neurotoxicity in the brain of mice exposed to arsenic at environmentally relevant levels. Journal of occupational health *47*, 445-449.

Purcell-Huynh, D.A., Farese, R.V., Jr., Johnson, D.F., Flynn, L.M., Pierotti, V., Newland, D.L., Linton, M.F., Sanan, D.A., and Young, S.G. (1995). Transgenic mice expressing high levels of human apolipoprotein B develop severe atherosclerotic lesions in response to a high-fat diet. The Journal of clinical investigation *95*, 2246-2257.

Rodier, F., and Campisi, J. (2011). Four faces of cellular senescence. The Journal of cell biology *192*, 547-556.

Rodier, F., Coppe, J.P., Patil, C.K., Hoeijmakers, W.A., Munoz, D.P., Raza, S.R., Freund, A., Campeau, E., Davalos, A.R., and Campisi, J. (2009). Persistent DNA damage signalling triggers senescence-associated inflammatory cytokine secretion. Nature cell biology *11*, 973-979.

Rossi, F.M., Guicherit, O.M., Spicher, A., Kringstein, A.M., Fatyol, K., Blakely, B.T., and Blau, H.M. (1998). Tetracycline-regulatable factors with distinct dimerization domains allow reversible growth inhibition by p16. Nature genetics *20*, 389-393.

Rovillain, E., Mansfield, L., Caetano, C., Alvarez-Fernandez, M., Caballero, O.L., Medema, R.H., Hummerich, H., and Jat, P.S. (2011). Activation of nuclear factor-kappa B signalling promotes cellular senescence. Oncogene *30*, 2356-2366.

Sager, R. (1991). Senescence as a mode of tumor suppression. Environmental health perspectives *93*, 59-62.

Sandrini, J.Z., Bianchini, A., Trindade, G.S., Nery, L.E., and Marins, L.F. (2009). Reactive oxygen species generation and expression of DNA repair-related genes after copper exposure in zebrafish (Danio rerio) ZFL cells. Aquat Toxicol *95*, 285-291.

Scharffetter-Kochanek, K., Brenneisen, P., Wenk, J., Herrmann, G., Ma, W., Kuhr, L., Meewes, C., and Wlaschek, M. (2000). Photoaging of the skin from phenotype to mechanisms. Experimental gerontology *35*, 307-316.

Schulze, M.B., Manson, J.E., Ludwig, D.S., Colditz, G.A., Stampfer, M.J., Willett, W.C., and Hu, F.B. (2004). Sugar-sweetened beverages, weight gain, and incidence of type 2 diabetes in young and middle-aged women. JAMA : the journal of the American Medical Association *292*, 927-934.

Serrano, M., Lin, A.W., McCurrach, M.E., Beach, D., and Lowe, S.W. (1997). Oncogenic ras provokes premature cell senescence associated with accumulation of p53 and p16INK4a. Cell *88*, 593-602.

Setlow, R.B., and Carrier, W.L. (1966). Pyrimidine dimers in ultraviolet-irradiated DNA's. Journal of molecular biology *17*, 237-254.

Shallo, H., Plackett, T.P., Heinrich, S.A., and Kovacs, E.J. (2003). Monocyte chemoattractant protein-1 (MCP-1) and macrophage infiltration into the skin after burn injury in aged mice. Burns : journal of the International Society for Burn Injuries *29*, 641-647.

Sharpless, N.E., and DePinho, R.A. (2007). How stem cells age and why this makes us grow old. Nature reviews Molecular cell biology *8*, 703-713.

Shi, Q., Hubbard, G.B., Kushwaha, R.S., Rainwater, D., Thomas, C.A., 3rd, Leland, M.M., Vandeberg, J.L., and Wang, X.L. (2007). Endothelial senescence after high-cholesterol, high-fat diet challenge in baboons. American journal of physiology Heart and circulatory physiology *292*, H2913-2920.

Signer, R.A., Montecino-Rodriguez, E., Witte, O.N., and Dorshkind, K. (2008). Aging and cancer resistance in lymphoid progenitors are linked processes conferred by p16Ink4a and Arf. Genes & development *22*, 3115-3120.

Singer, A.J., and Clark, R.A. (1999). Cutaneous wound healing. The New England journal of medicine *341*, 738-746.

Slikker, W., Jr., Xu, Z.A., Levin, E.D., and Slotkin, T.A. (2005). Mode of action: disruption of brain cell replication, second messenger, and neurotransmitter systems during

development leading to cognitive dysfunction--developmental neurotoxicity of nicotine. Critical reviews in toxicology *35*, 703-711.

Smith, A.H., Hopenhayn-Rich, C., Bates, M.N., Goeden, H.M., Hertz-Picciotto, I., Duggan, H.M., Wood, R., Kosnett, M.J., and Smith, M.T. (1992). Cancer risks from arsenic in drinking water. Environmental health perspectives *97*, 259-267.

Sohal, R.S., Ku, H.H., Agarwal, S., Forster, M.J., and Lal, H. (1994). Oxidative damage, mitochondrial oxidant generation and antioxidant defenses during aging and in response to food restriction in the mouse. Mechanisms of ageing and development *74*, 121-133.

Sone, H., and Kagawa, Y. (2005). Pancreatic beta cell senescence contributes to the pathogenesis of type 2 diabetes in high-fat diet-induced diabetic mice. Diabetologia *48*, 58-67.

Song, Z., von Figura, G., Liu, Y., Kraus, J.M., Torrice, C., Dillon, P., Rudolph-Watabe, M., Ju, Z., Kestler, H.A., Sanoff, H., *et al.* (2010). Lifestyle impacts on the aging-associated expression of biomarkers of DNA damage and telomere dysfunction in human blood. Aging cell *9*, 607-615.

Stone, S., Dayananth, P., and Kamb, A. (1996). Reversible, p16-mediated cell cycle arrest as protection from chemotherapy. Cancer research *56*, 3199-3202.

Taaffe, D.R., Harris, T.B., Ferrucci, L., Rowe, J., and Seeman, T.E. (2000). Cross-sectional and prospective relationships of interleukin-6 and C-reactive protein with physical performance in elderly persons: MacArthur studies of successful aging. The journals of gerontology Series A, Biological sciences and medical sciences *55*, M709-715.

Tannenbaum, A. (1942). The genesis and growth of tumors III Effects of a high-fat diet. Cancer research *12*, 468-475.

Tchkonia, T., Morbeck, D.E., Von Zglinicki, T., Van Deursen, J., Lustgarten, J., Scrable, H., Khosla, S., Jensen, M.D., and Kirkland, J.L. (2010). Fat tissue, aging, and cellular senescence. Aging cell *9*, 667-684.

Telgenhoff, D., and Shroot, B. (2005). Cellular senescence mechanisms in chronic wound healing. Cell death and differentiation *12*, 695-698.

Theocharis, S., Kouraklis, G., Margeli, A., Agapitos, E., Ninos, S., Karatzas, G., and Koutselinis, A. (2003). Glucocorticoid receptor (GR) immunohistochemical expression is correlated with cell cycle-related molecules in human colon cancer. Digestive diseases and sciences *48*, 1745-1750.

Tilstra, J.S., Robinson, A.R., Wang, J., Gregg, S.Q., Clauson, C.L., Reay, D.P., Nasto, L.A., St Croix, C.M., Usas, A., Vo, N., *et al.* (2012). NF-kappaB inhibition delays DNA damage-induced senescence and aging in mice. The Journal of clinical investigation *122*, 2601-2612.

Tong, Z., Han, C., Luo, W., Li, H., Luo, H., Qiang, M., Su, T., Wu, B., Liu, Y., Yang, X., *et al.* (2013). Aging-associated excess formaldehyde leads to spatial memory deficits. Scientific reports *3*, 1807.

Tran, H.P., Prakash, A.S., Barnard, R., Chiswell, B., and Ng, J.C. (2002). Arsenic inhibits the repair of DNA damage induced by benzo(a)pyrene. Toxicology letters *133*, 59-67.

Valdes, A.M., Andrew, T., Gardner, J.P., Kimura, M., Oelsner, E., Cherkas, L.F., Aviv, A., and Spector, T.D. (2005). Obesity, cigarette smoking, and telomere length in women. Lancet *366*, 662-664.

Visel, A., Zhu, Y., May, D., Afzal, V., Gong, E., Attanasio, C., Blow, M.J., Cohen, J.C., Rubin, E.M., and Pennacchio, L.A. (2010). Targeted deletion of the 9p21 non-coding coronary artery disease risk interval in mice. Nature *464*, 409-412.

Wang, C.Y., Kim, H.H., Hiroi, Y., Sawada, N., Salomone, S., Benjamin, L.E., Walsh, K., Moskowitz, M.A., and Liao, J.K. (2009). Obesity increases vascular senescence and susceptibility to ischemic injury through chronic activation of Akt and mTOR. Science signaling *2*, ra11.

Wang, X.Q., Gabrielli, B.G., Milligan, A., Dickinson, J.L., Antalis, T.M., and Ellem, K.A. (1996). Accumulation of p16CDKN2A in response to ultraviolet irradiation correlates with late S-G(2)-phase cell cycle delay. Cancer research *56*, 2510-2514.

Wang, Y., Schulte, B.A., LaRue, A.C., Ogawa, M., and Zhou, D. (2006). Total body irradiation selectively induces murine hematopoietic stem cell senescence. Blood *107*, 358-366.

Wei, H., Ca, Q., Rahn, R., Zhang, X., Wang, Y., and Lebwohl, M. (1998). DNA structural integrity and base composition affect ultraviolet light-induced oxidative DNA damage. Biochemistry *37*, 6485-6490.

Wilkinson, J.E., Burmeister, L., Brooks, S.V., Chan, C.C., Friedline, S., Harrison, D.E., Hejtmancik, J.F., Nadon, N., Strong, R., Wood, L.K., *et al.* (2012). Rapamycin slows aging in mice. Aging cell *11*, 675-682.

Winzell, M.S., and Ahren, B. (2004). The high-fat diet-fed mouse: a model for studying mechanisms and treatment of impaired glucose tolerance and type 2 diabetes. Diabetes *53 Suppl 3*, S215-219.

Wu, M.M., Chiou, H.Y., Wang, T.W., Hsueh, Y.M., Wang, I.H., Chen, C.J., and Lee, T.C. (2001). Association of blood arsenic levels with increased reactive oxidants and decreased antioxidant capacity in a human population of northeastern Taiwan. Environmental health perspectives *109*, 1011-1017.

Xu, X.H., Shah, P.K., Faure, E., Equils, O., Thomas, L., Fishbein, M.C., Luthringer, D., Xu, X.P., Rajavashisth, T.B., Yano, J., *et al.* (2001). Toll-like receptor-4 is expressed by macrophages in murine and human lipid-rich atherosclerotic plaques and upregulated by oxidized LDL. Circulation *104*, 3103-3108.

Yamauchi, H., Aminaka, Y., Yoshida, K., Sun, G., Pi, J., and Waalkes, M.P. (2004). Evaluation of DNA damage in patients with arsenic poisoning: urinary 8-hydroxydeoxyguanine. Toxicology and applied pharmacology *198*, 291-296.

Yang, F., Tuxhorn, J.A., Ressler, S.J., McAlhany, S.J., Dang, T.D., and Rowley, D.R. (2005). Stromal expression of connective tissue growth factor promotes angiogenesis and prostate cancer tumorigenesis. Cancer research *65*, 8887-8895.

Zhu, J., Woods, D., McMahon, M., and Bishop, J.M. (1998). Senescence of human fibroblasts induced by oncogenic Raf. Genes & development *12*, 2997-3007.

Zindy, F., Quelle, D.E., Roussel, M.F., and Sherr, C.J. (1997). Expression of the p16INK4a tumor suppressor versus other INK4 family members during mouse development and aging. Oncogene *15*, 203-211.